N73-15986

NASA TM X-2703

NASA TECHNICAL MEMORANDUM

NASA TM X-2703

CASE FILE COPY

SUPERSONIC AERODYNAMIC CHARACTERISTICS OF A VARIABLE-GEOMETRY SPACECRAFT DESIGNED FOR HIGH HYPERSONIC PERFORMANCE

by Bernard Spencer, Jr., and Roger H. Fournier

Langley Research Center
Hampton, Va. 23365

NATIONAL AERONAUTICS AND SPACE ADMINISTRATION • WASHINGTON, D. C. • JANUARY 1973

1. Report No.	2. Government Accession No.	3. Recipient's Catalog No.
NASA TM X-2703		

4. Title and Subtitle	5. Report Date
SUPERSONIC AERODYNAMIC CHARACTERISTICS OF A VARIABLE-GEOMETRY SPACECRAFT DESIGNED FOR HIGH HYPERSONIC PERFORMANCE	January 1973
	6. Performing Organization Code
7. Author(s)	8. Performing Organization Report No.
Bernard Spencer, Jr., and Roger H. Fournier	L-8639
9. Performing Organization Name and Address	10. Work Unit No.
NASA Langley Research Center Hampton, Va. 23365	502-37-01-01
	11. Contract or Grant No.
12. Sponsoring Agency Name and Address	13. Type of Report and Period Covered
National Aeronautics and Space Administration Washington, D.C. 20546	Technical Memorandum
	14. Sponsoring Agency Code

15. Supplementary Notes

16. Abstract

An investigation has been made in the high Mach number test section of the Langley Unitary Plan wind tunnel on a variable-geometry high hypersonic performance spacecraft concept at Mach numbers from 2.30 to 4.63. The basic lifting body is designed for hypersonic lift-drag ratio near 3.0. The variable-geometry feature is a single-pivot two-position high wing which is deployed at subsonic speeds to improve vehicle landing characteristics. For the present investigation the wing was maintained in a stowed position, and the effects of horizontal stabilizer dihedral, elevon control effectiveness, and the addition of either a conventional single vertical tail or dorsal-fin-type vertical stabilizers on the longitudinal and lateral-directional stability and control characteristics were studied.

17. Key Words (Suggested by Author(s))	18. Distribution Statement
Variable-geometry spacecraft High hypersonic performance Logistics vehicle	Unclassified – Unlimited

19. Security Classif. (of this report)	20. Security Classif. (of this page)	21. No. of Pages	22. Price*
Unclassified	Unclassified	46	$3.00

*For sale by the National Technical Information Service, Springfield, Virginia 22151

SUPERSONIC AERODYNAMIC CHARACTERISTICS OF A VARIABLE-GEOMETRY SPACECRAFT DESIGNED FOR HIGH HYPERSONIC PERFORMANCE

By Bernard Spencer, Jr., and Roger H. Fournier
Langley Research Center

SUMMARY

An investigation has been made in the high Mach number test section of the Langley Unitary Plan wind tunnel on a variable-geometry high hypersonic performance spacecraft concept at Mach numbers from 2.30 to 4.63. The basic lifting body is designed for hypersonic lift-drag ratio near 3.0. The variable-geometry feature is a single-pivot two-position high wing which is deployed at subsonic speeds to improve vehicle landing characteristics. For the present investigation the wing was maintained in a stowed position, and the effects of horizontal stabilizer dihedral, elevon control effectiveness, and the addition of either a conventional single vertical tail or dorsal-fin-type vertical stabilizers on the longitudinal and lateral-directional stability and control characteristics were studied.

A comparison of the untrimmed maximum lift-drag ratio for the configurations having horizontal-tail dihedral of 0° and either a center-line vertical tail or dorsal fins indicates slightly higher values for the dorsal-fin configuration at Mach numbers from 2.30 to 4.63, whereas comparison of trimmed maximum lift-drag ratio for these configurations indicates considerably higher values for the center-line vertical tail, especially at the lower Mach numbers.

Positive effective dihedral and directional stability were noted for each configuration near the angle of attack for maximum trimmed lift-drag ratio; large decreases in both parameters accompany increases in Mach number.

INTRODUCTION

The National Aeronautics and Space Administration, Department of Defense, and industry have studied numerous concepts relating to the development of manned orbital spacecraft suitable for supporting an orbiting near-earth laboratory, as well as independent missions in space. Criteria established for these advanced concepts are that lifting entry (that is, some cross-range capability) is desired along with the requirement for horizontal landing on conventional runways as the final mode of recovery. Although

primary interest was centered on fixed-wing body configurations, some studies of lifting entry vehicles (ref. 1) have also considered the inclusion of variable-geometry features in the form of conventional wings which are stowed or shielded during entry and deployed at some point along the return flight path to improve the overall aerodynamic behavior and performance for landing. In reference 1 a spectrum of variable-geometry vehicles was investigated, in-depth analysis being performed on six concepts. Two vehicles were studied in each of the three hypersonic lift-drag-ratio categories of near 1.0, 2.0, and 3.0. In addition, the dynamic flight characteristics and handling qualities of the most promising vehicle in each of the hypersonic lift-drag-ratio 1.0, 2.0, and 3.0 categories, each having some form of variable-geometry feature, were studied. (See refs. 2 to 4.) Extensive wind-tunnel studies from low subsonic to hypersonic speeds were made for these selected concepts to provide a realistic data base for inclusion in the dynamic estimates. These vehicles were sized for small payloads but the associated aerodynamics determined for each of these diverse designs should prove beneficial to the design of larger payload advanced entry or hypersonic transport concepts.

The purpose of this paper is to present supersonic aerodynamic results on the lift-drag-ratio-3.0 class vehicle studied in the efforts previously described. A single-pivot two-position wing was employed as the variable-geometry feature for this vehicle. Transonic characteristics of this vehicle are presented in reference 5. The wing is stowed near the top of the body during entry and high-speed flight and deployed at subsonic speeds to improve the landing characteristics. The basic body is trapezoidal in cross section with an upper to lower surface ratio of 1 to 3, and has a longitudinal area distribution conforming to that required to minimize zero-lift hypersonic wave drag as determined under the geometric constraints of given length and volume. (See refs. 6 and 7.) Effective fineness ratio of the body is 6.0 with a ratio of volume to length cubed of 0.0110. Horizontal stabilizers and dorsal-type vertical fins are located in the aft part of the body to provide longitudinal and lateral-directional stability with longitudinal and roll control provided by elevons located on the horizontal stabilizers. A single center vertical tail was also tested with several horizontal stabilizer configurations. The present tests were made in the high Mach number test section of the Langley Unitary Plan wind tunnel at Mach numbers of 2.30, 2.96, 3.96, and 4.63. The supersonic aerodynamic characteristics associated with the basic body with wings stowed, and horizontal stabilizers at various dihedral positions with and without dorsal fins or a center vertical tail were studied. Horizontal stabilizer elevon control effectiveness was also studied at stabilizer dihedral angles of 0° and $\pm 30^{\circ}$.

SYMBOLS

Longitudinal aerodynamic characteristics are referenced to the stability system of axes and lateral-directional characteristics are presented about the body axes. All coefficients are normalized with respect to the projected planform area, actual length, and span of the basic body. The moment reference point was located longitudinally at 62.8 percent of body length as measured from the body apex, with the vertical location of the moment reference point at 3.29 percent body length below the model reference plane. Values are given in both SI and U.S. Customary Units. The measurements and calculations were made in U.S. Customary Units.

a_1 lower surface semiwidth of body at station x, m (ft)

a_2 upper surface semiwidth of body at station x, m (ft)

b maximum span of body, 0.228 m (0.750 ft)

C_D drag coefficient, $\frac{\text{Drag}}{q_\infty S}$

C_L lift coefficient, $\frac{\text{Lift}}{q_\infty S}$

C_{L_α} lift-curve slope, $\frac{\partial C_L}{\partial \alpha}$ at $\alpha = 0^\circ$, per degree

C_l rolling-moment coefficient, $\frac{\text{Rolling moment}}{q_\infty Sb}$

C_{l_β} lateral stability parameter, $\frac{\Delta C_l}{\Delta \beta}$ at $\beta = 0^\circ$ and 5°, per degree

C_m pitching-moment coefficient, $\frac{\text{Pitching moment}}{q_\infty Sl}$

C_n yawing-moment coefficient, $\frac{\text{Yawing moment}}{q_\infty Sb}$

C_{n_β} directional stability parameter, $\frac{\Delta C_n}{\Delta \beta}$ at $\beta = 0^\circ$ and 5°, per degree

$C_{p,b}$ base pressure coefficient, $\frac{p_b - p_\infty}{q_\infty}$

C_Y side-force coefficient, $\frac{\text{Side force}}{q_\infty S}$

C_{Y_β} side-force parameter, $\frac{\Delta C_Y}{\Delta \beta}$ at $\beta = 0^\circ$ and 5°, per degree

h body height at station x, m (ft)

L/D lift-drag ratio

l length of body, 0.965 m (3.167 ft)

M Mach number

p_b base pressure, N/m^2 (lb/ft^2)

p_∞ free-stream static pressure, N/m^2 (lb/ft^2)

q_∞ free-stream dynamic pressure, N/m^2 (lb/ft^2)

S body projected planform area, 0.144 m^2 (1.545 ft^2)

x longitudinal coordinate of body, m (ft)

α angle of attack, deg

β angle of sideslip, deg

Γ_t horizontal-tail dihedral angle (positive up), deg

Γ_v dorsal-fin dihedral angle (positive up) ($\Gamma_v = 90^\circ$ designates single center-line tail and $\Gamma_v = 45^\circ$ designates twin dorsal fins), deg

δ_e horizontal-tail elevon deflection angle (positive with trailing edge down), deg

Subscripts:

max maximum condition

min minimum condition

o condition at $\alpha = 0^\circ$

trim trimmed condition

Configuration designations:

B	body
H	horizontal stabilizers
V_c	center-line vertical tail
V_t	dorsal fins

MODEL

A drawing of the complete model is shown in figure 1, and a photograph of the model is presented in figure 2. Table I presents body ordinates normalized with respect to body length.

The body is trapezoidal in cross section with a ratio of top to bottom of 1 to 3. Negative camber was incorporated in the body by placing 0.333 of the vertical height above and 0.667 of the vertical height below the model reference plane at all longitudinal stations. The large blunt base was retained (no boattailing) for efficient spacecraft-booster integration (tandem launch being assumed) or to provide the area required for rocket engine housing on shuttle type or advanced transport concepts.

The horizontal stabilizers were located along the lower body ridge line just ahead of the base region and were tested at dihedral angles of 30°, 0°, and -30°. The stabilizers for these tests had rounded leading edges with 2° (included angle) wedge airfoil sections, no incidence, and 65° leading-edge sweep. Elevon controls located on these stabilizers were tested at deflections of 0°, -10°, and -20° for pitch control and differentially for roll control about hinge lines located at the most aft body station. (See fig. 1.) Total exposed horizontal stabilizer area including the elevons was 18.74 percent of the body planform area. Dorsal fins were located on the sides of the body and were tested at a dihedral angle of 45° as measured from the horizontal reference plane. (See fig. 1.) Total exposed area for these dorsal fins was also 18.74 percent of the body planform area. A single center-line vertical tail was also tested with several horizontal stabilizer configurations; the tail had a flat-plate cross section with rounded leading edge and blunt base. For the present investigation the wing was considered to be stowed.

TEST AND CORRECTIONS

The investigation was made in the high Mach number test section of the Langley Unitary Plan wind tunnel. The tunnel is a variable-pressure return-flow type with a

test section approximately 1.22 m (4 ft) square and 2.13 m (7 ft) long. The nozzle leading to the test section has an asymmetric sliding block which permits variation of Mach number from 2.30 to 4.63.

The model was sting supported and forces and moments were measured by use of an internally mounted strain-gage balance. Static-pressure measurements were also taken at the base of the model.

The tests were made through an angle-of-attack range from about -5° to 21° at sideslip angles of 0° and 5° and at a constant Reynolds number of 8.7×10^{6} (based on body length). All angles of attack and sideslip have been corrected for deflection of the balance and sting due to aerodynamic loads. The angle of attack was also corrected for tunnel-flow misalinement. Static-pressure measurements taken at the base of the model are presented in the form of pressure coefficients in figure 3. The drag results presented herein, however, represent gross drag in that the axial force is uncorrected for the base pressure.

The Mach numbers, stagnation pressures, and stagnation temperatures were as follows:

M	Stagnation pressure		Stagnation temperature	
	kN/m^2	lb/ft^2 abs	K	$^{\circ}F$
2.30	100.60	2101	338	150
2.96	142.30	2972	338	150
3.96	253.48	5294	352	175
4.63	345.98	7226	352	175

Stagnation dewpoint was maintained sufficiently low (238 K or -30° F) to insure that no condensation effects would be encountered in the test section.

RESULTS AND DISCUSSION

Longitudinal aerodynamic characteristics are presented in figures 4 to 8 and are summarized in figures 9 and 10. Summary lateral-directional stability characteristics are presented in figures 11 and 12. The following index is presented as an aid in locating a particular set of data:

	Figure
Longitudinal characteristics of various vehicle components	4
Longitudinal control characteristics for –	
$\Gamma_t = 0^{\circ}$; $\Gamma_v = 90^{\circ}$	5
$\Gamma_t = -30^{\circ}$; $\Gamma_v = 90^{\circ}$	6

Figure

$\Gamma_t = 30^o$; $\Gamma_v = 90^o$ 7

$\Gamma_t = 0^o$; $\Gamma_v = 45^o$ 8

Summary of untrimmed longitudinal aerodynamic characteristics 9

Summary of lateral-directional stability characteristics of various configurations 10

Summary of lateral-directional stability characteristics as affected by horizontal-stabilizer dihedral 11

Summary of trimmed longitudinal and lateral-directional aerodynamic characteristics 12

Longitudinal Characteristics

A summary of the untrimmed longitudinal characteristics for various configurations is presented in figure 9. The addition of the center-line vertical tail increased $C_{D,min}$ with attendant losses in $(L/D)_{max}$ as would be expected. It is interesting to note the favorable increase in positive $C_{m,o}$ resulting from addition of this tail. (See fig. 9(a).) Addition of the dorsal fins while increasing $C_{D,min}$ also increased $(L/D)_{max}$ as a result of the improved C_{L_α} characteristics. (See fig. 9(b).) These fins also increase positive $C_{m,o}$ but not as significantly as that associated with the center-line vertical tail.

The addition of the horizontal stabilizers at $\Gamma_t = 0^o$ to the configuration having center-line vertical tail resulted in increases in untrimmed $(L/D)_{max}$ at the lower Mach numbers, a reduction being noted above $M = 3.6$ (fig. 9(a)), whereas adding these stabilizers to the configuration with dorsal fins increased $(L/D)_{max}$ at all test Mach numbers. Large increases in the longitudinal stability parameter $\partial C_m/\partial C_L$ were noted by addition of the stabilizer ($\Gamma_t = 0^o$) to the configuration having center-line vertical tail (fig. 9(a)). For the body-dorsal-fin configuration, however, only slight increases in $\partial C_m/\partial C_L$ over that already provided by the addition of the dorsal fins resulted from addition of the horizontal stabilizer ($\Gamma_t = 0^o$; fig. 9(b)). A comparison of the untrimmed $(L/D)_{max}$ values for BV_cH and BV_tH configurations ($\Gamma_t = 0^o$) indicates slightly higher values for BV_tH at all Mach numbers.

Summary of Lateral-Directional Stability Characteristics

The effects of the addition of various configuration components on the lateral-directional stability are presented in figure 10. Addition of the center-line vertical tail showed large increases in C_{n_β} at the lower angles of attack, large decreases occurring with increasing α. Considerable reduction in C_{n_β}, however, occurs as Mach number is increased even near $\alpha = 0^o$ (that is, from $C_{n_\beta} = 0.0052$ at $M = 2.30$ to 0.001 at

$M = 4.63$). Addition of the dorsal fins indicates the largest increases in C_{n_β} to occur at the higher angles of attack at all Mach numbers. Again considerable reduction in C_{n_β} occurs as Mach number is increased (that is, at $\alpha = 18^\circ$ from $C_{n_\beta} = 0.007$ at $M = 2.30$ to $C_{n_\beta} = 0.0025$ at $M = 4.63$). The addition of either the center-line vertical or dorsal fin resulted in positive effective dihedral $\left(-C_{l_\beta}\right)$ at all test angles of attack and Mach numbers.

The addition of the horizontal tail at $\Gamma_t = 0^\circ$ to either the center-line or dorsal-fin configurations showed only minor effects on C_{n_β}. The horizontal tails, however, did have a destabilizing effect on C_{l_β} at angles of attack generally below 5° at all test Mach numbers.

The effects of horizontal-tail dihedral on lateral-directional stability are presented in figure 11. Changing dihedral from $\Gamma_t = 0^\circ$ to $\Gamma_t = -30^\circ$ resulted in large increases in C_{n_β} at moderate α (that is, below $\alpha \approx 12^\circ$) at all Mach numbers. This favorable effect diminishes rapidly, however, with increasing α. Regions of unfavorable effective dihedral parameter C_{l_β} were noted to occur for this configuration generally below $\alpha \approx 6^\circ$ at all Mach numbers. Increasing dihedral from $\Gamma_t = 0^\circ$ to $\Gamma_t = 30^\circ$ indicates a reduction in C_{n_β} near $\alpha = 0^\circ$ and a favorable increase in C_{n_β} at the higher angles of attack at all Mach numbers. No regions of unfavorable C_{l_β} were noted to occur for this configuration.

Summary of Trimmed Characteristics

A summary of the trimmed $(L/D)_{max}$ and α at trimmed $(L/D)_{max}$ for the various configurations is presented in figure 12. Higher values of trimmed $(L/D)_{max}$ were obtained on the configuration having a center-line vertical tail with $\Gamma_t = 0^\circ$ or $\Gamma_t = -30^\circ$ as compared with the dorsal-fin configuration having $\Gamma_t = 0^\circ$ at all Mach numbers (the largest increases being noted at the lowest Mach numbers). The BV_cH ($\Gamma_t = 30^\circ$) configuration, although it indicated slightly higher values of trimmed $(L/D)_{max}$ at $M \leqq 2.86$, was out of trim positively for the elevon settings tested at $M > 2.86$; thus, a down-elevon would be required for trim. This condition results from the higher $C_{m,o}$ values for the $\Gamma_t = 30^\circ$ configurations and the decreasing longitudinal stability variation with increasing angle of attack, especially at the higher test Mach numbers. (For example, see fig. 7.) All configurations were directionally stable and had positive effective dihedral in the region of trimmed $(L/D)_{max}$ at all Mach numbers. (See fig. 12.)

CONCLUDING REMARKS

An investigation has been made in the high Mach number test section of the Langley Unitary Plan wind tunnel on a variable-geometry high hypersonic performance spacecraft concept at Mach numbers from 2.30 to 4.63. The basic lifting body is designed for

hypersonic lift-drag ratio near 3.0. The variable-geometry feature is a single-pivot two-position high wing which is deployed at subsonic speeds to improve vehicle landing characteristics. For the present investigation the wing was maintained in a stowed position, and the effects of horizontal stabilizer dihedral, elevon control effectiveness, and the addition of either a conventional single vertical-tail or dorsal-fin-type vertical stabilizers on the longitudinal and lateral-directional stability and control characteristics were studied. Some observations of this study are presented:

A comparison of the untrimmed maximum lift-drag ratio for the configurations having horizontal-tail dihedral of 0° and either a center-line vertical tail or dorsal fins indicates slightly higher values for the dorsal-fin configuration at Mach numbers from 2.30 to 4.63, whereas a comparison of trimmed maximum lift-drag ratio for these configurations indicates considerably higher values for the center-line vertical tail, especially at the lower Mach numbers.

Positive effective dihedral and directional stability were noted for each configuration near the angle of attack for maximum trimmed lift-drag ratio; large decreases in both parameters accompany increases in Mach number.

Langley Research Center,
National Aeronautics and Space Administration,
Hampton, Va., December 7, 1972.

REFERENCES

1. Anon.: A Study To Determine the Weight and Performance Characteristics of Variable Geometry Spacecraft. Volume I – Summary. GDC-DCB68-012 (Contract NAS 1-7675), Gen. Dyn./Convair, July 12, 1968. (Available as NASA CR-66685.)

2. Kuchta, B. J.: A Study To Determine Flight Characteristics and Handling Qualities of Variable Geometry Spacecraft. Volume I – High L/D Concept With Single Pivot Two-Position Skewed Wing. NASA CR-1545, 1970.

3. Kuchta, B. J.; and Friedman, G. R.: A Study To Determine Flight Characteristics and Handling Qualities of Variable Geometry Spacecraft. Volume II – Medium L/D Concept With Switch-Blade Wings. NASA CR-1789, 1972.

4. Friedman, G. R.; and Kuchta, B. J.: A Study To Determine Flight Characteristics and Handling Qualities of Variable Geometry Spacecraft. Volume III – Low L/D Concept With Fold-Down Wings. NASA CR-1890, 1972.

5. Spencer, Bernard, Jr.: Effects of Stabilizer Configuration on Transonic Aerodynamic Characteristics of a Variable-Geometry High-Hypersonic-Performance Spacecraft. NASA TM X-1865, 1969.

6. Spencer, Bernard, Jr.; and Fox, Charles H., Jr.: Hypersonic Aerodynamic Performance of Minimum-Wave-Drag Bodies. NASA TR R-250, 1966.

7. Spencer, Bernard, Jr.: Hypersonic Aerodynamic Characteristics of Minimum-Wave-Drag Bodies Having Variations in Cross-Sectional Shape. NASA TN D-4079, 1967.

TABLE I.- DESIGN BODY COORDINATES

x/l	a_1/l	a_2/l	h/l	$0.333h/l$	$0.667h/l$
0	0	0	0	0	0
.01	.00503	.00168	.00591	.00197	.00394
.02	.00794	.00265	.00936	.00312	.00624
.03	.01090	.00363	.01287	.00429	.00858
.04	.01349	.00450	.01590	.00530	.01060
.05	.01592	.00531	.01876	.00625	.01251
.06	.01826	.00609	.02151	.00717	.01434
.07	.02050	.00683	.02415	.00805	.01610
.08	.02270	.00757	.02675	.00892	.01784
.09	.02476	.00825	.02919	.00973	.01946
.10	.02775	.00925	.03271	.01090	.02180
.20	.04475	.01492	.05274	.01758	.03516
.30	.05953	.01984	.07015	.02337	.04676
.40	.07236	.02412	.08529	.02843	.05686
.50	.08402	.02801	.09900	.03300	.06600
.60	.09408	.03136	.01108	.03695	.07391
.70	.10269	.03423	.12101	.04034	.08067
.80	.11007	.03669	.12970	.04314	.08647
.90	.11547	.03849	.13607	.04535	.09071
.94	.11695	.03899	.13782	.04594	.09188
.96	.11757	.03919	.13855	.04618	.09237
.98	.11807	.03936	.13914	.04638	.09276
1.00	.11834	.03945	.13946	.04649	.09297

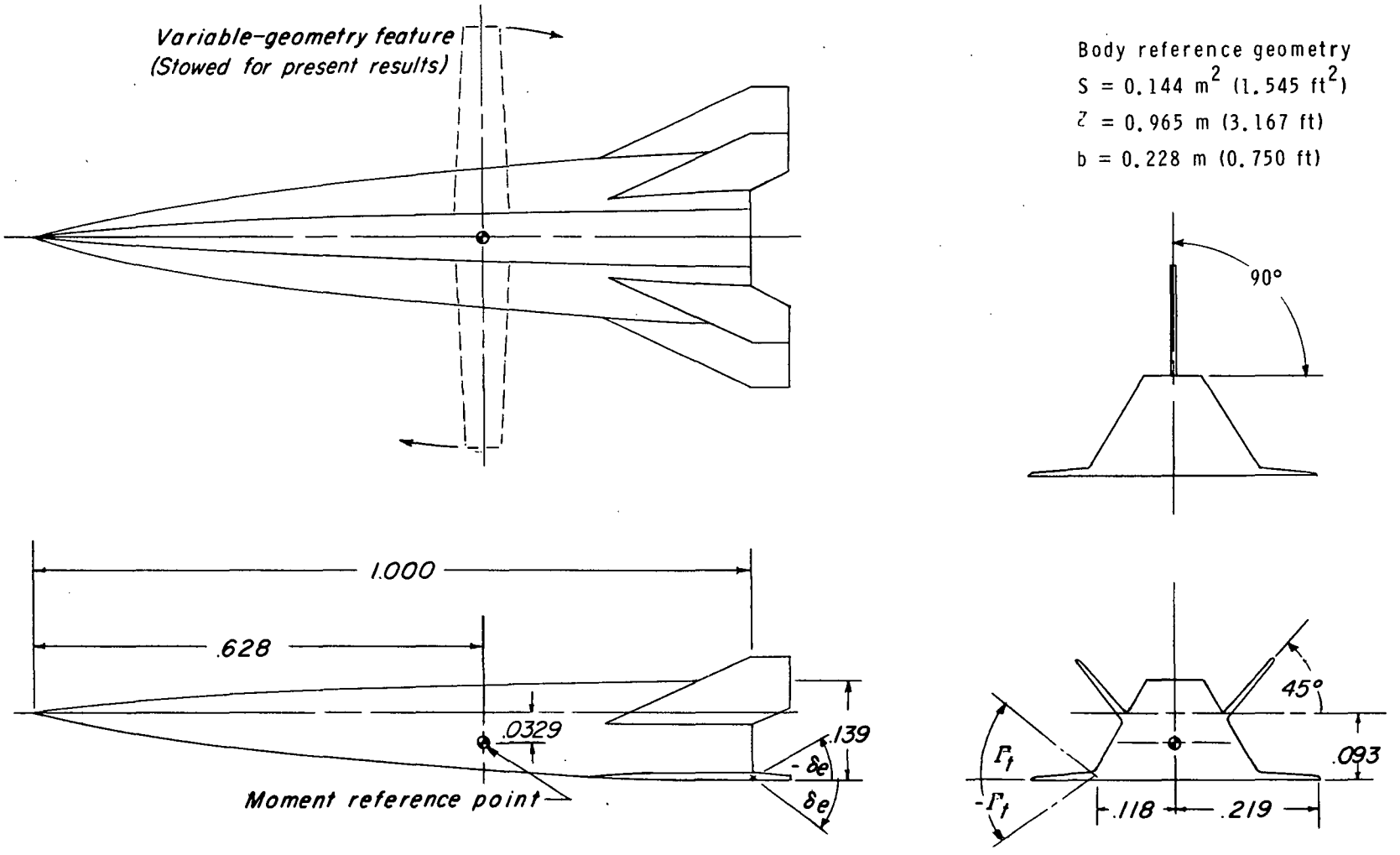

(a) Basic body with horizontal stabilizers and dorsal fins.

Figure 1.- Drawings of model of present investigation. All dimensions are normalized with respect to maximum body length.

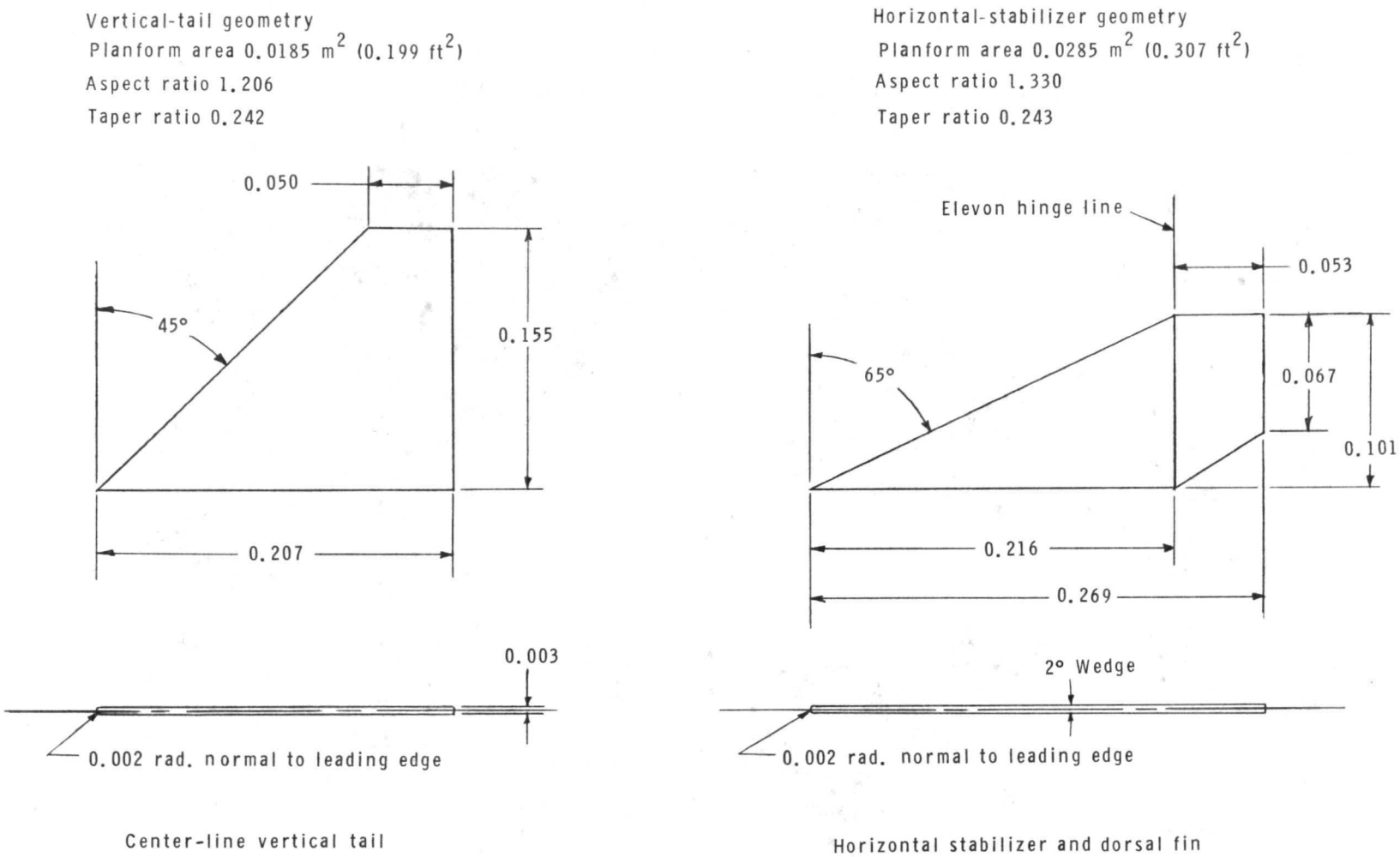

(b) Details of vertical tail and horizontal stabilizer and dorsal fin.

Figure 1.- Concluded.

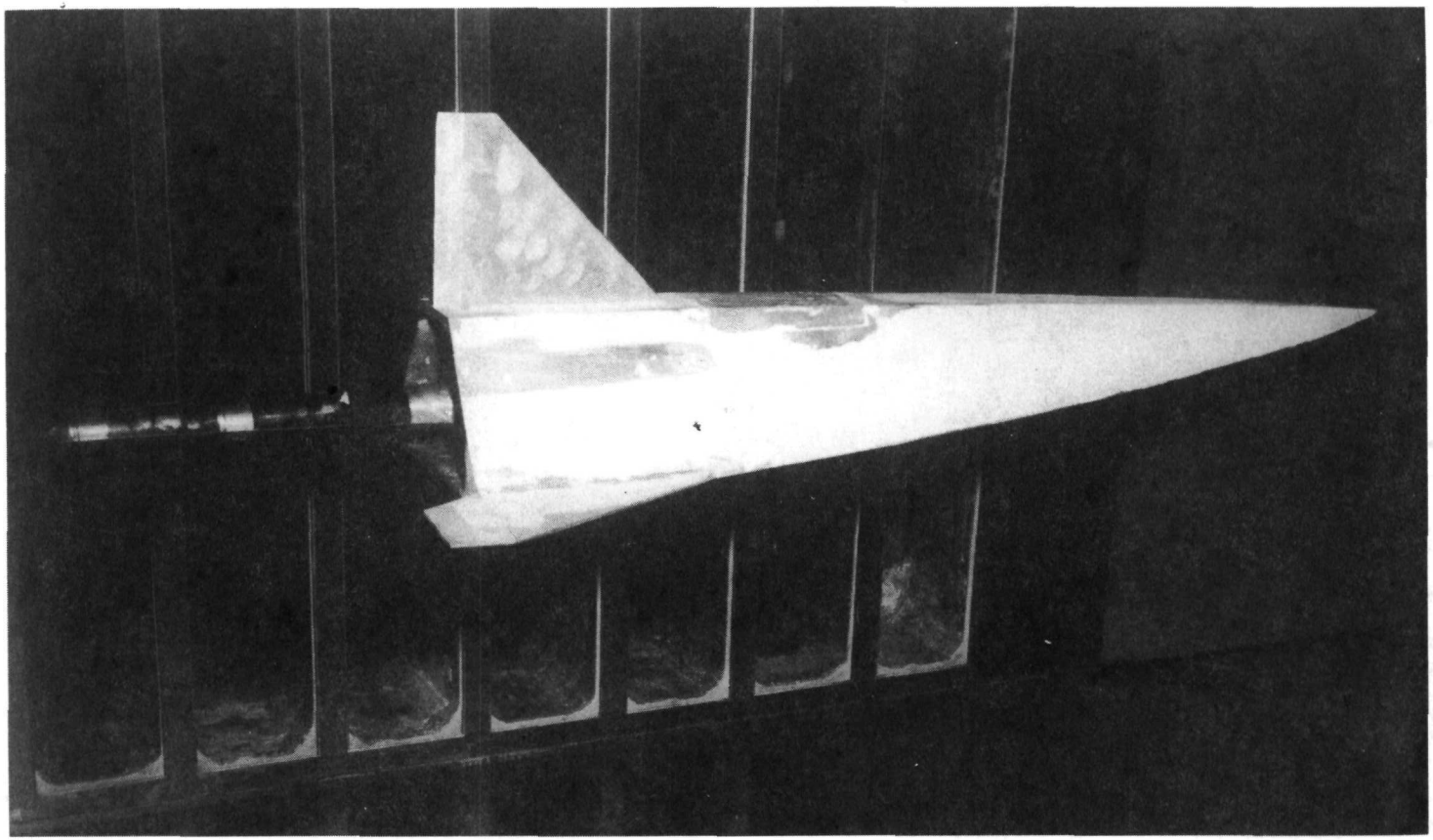

L-68-3357

Figure 2.- Typical model photograph. Center-line vertical tail.

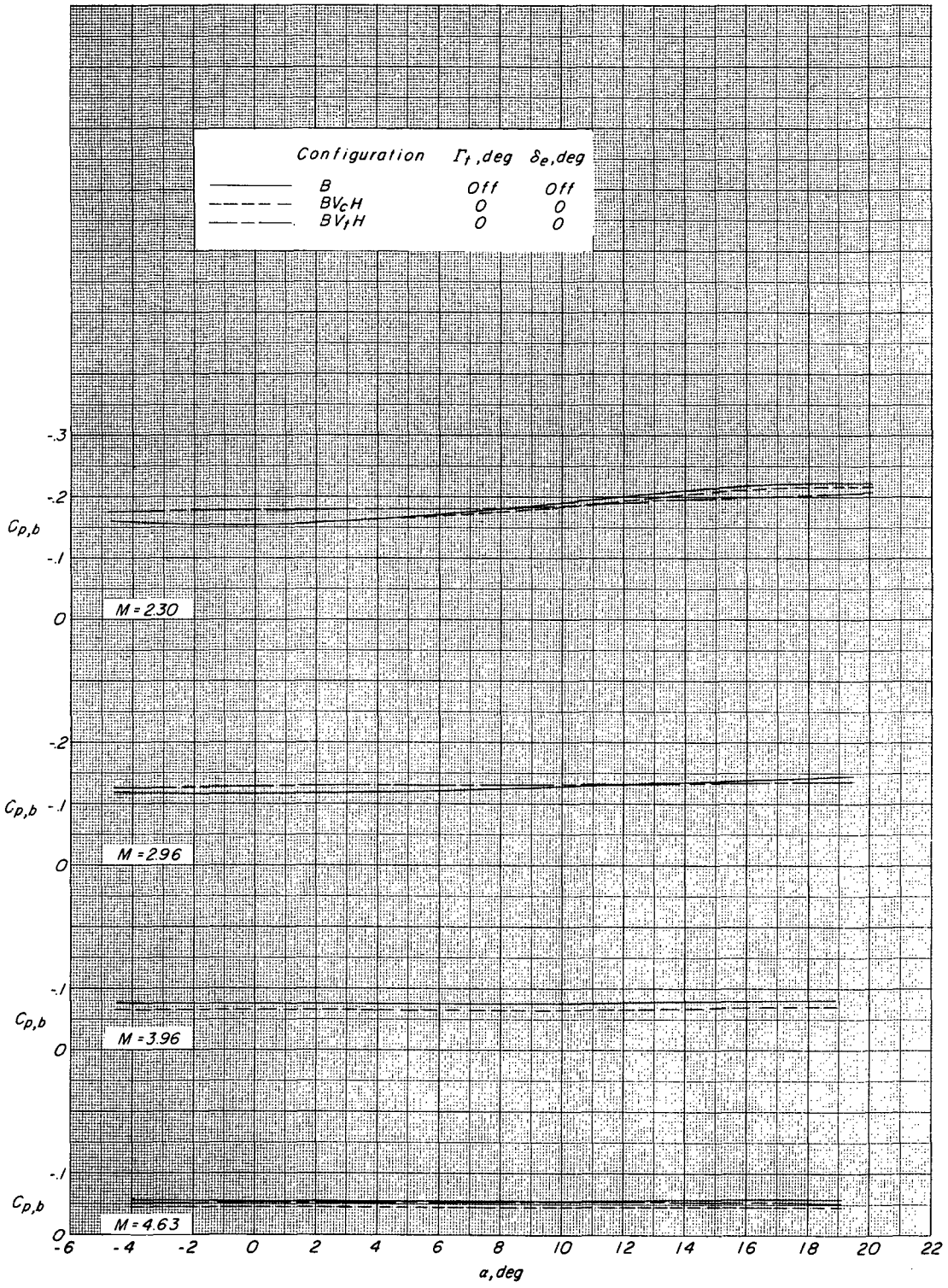

Figure 3.- Variation of base-pressure coefficient with angle of attack and Mach number for various configurations.

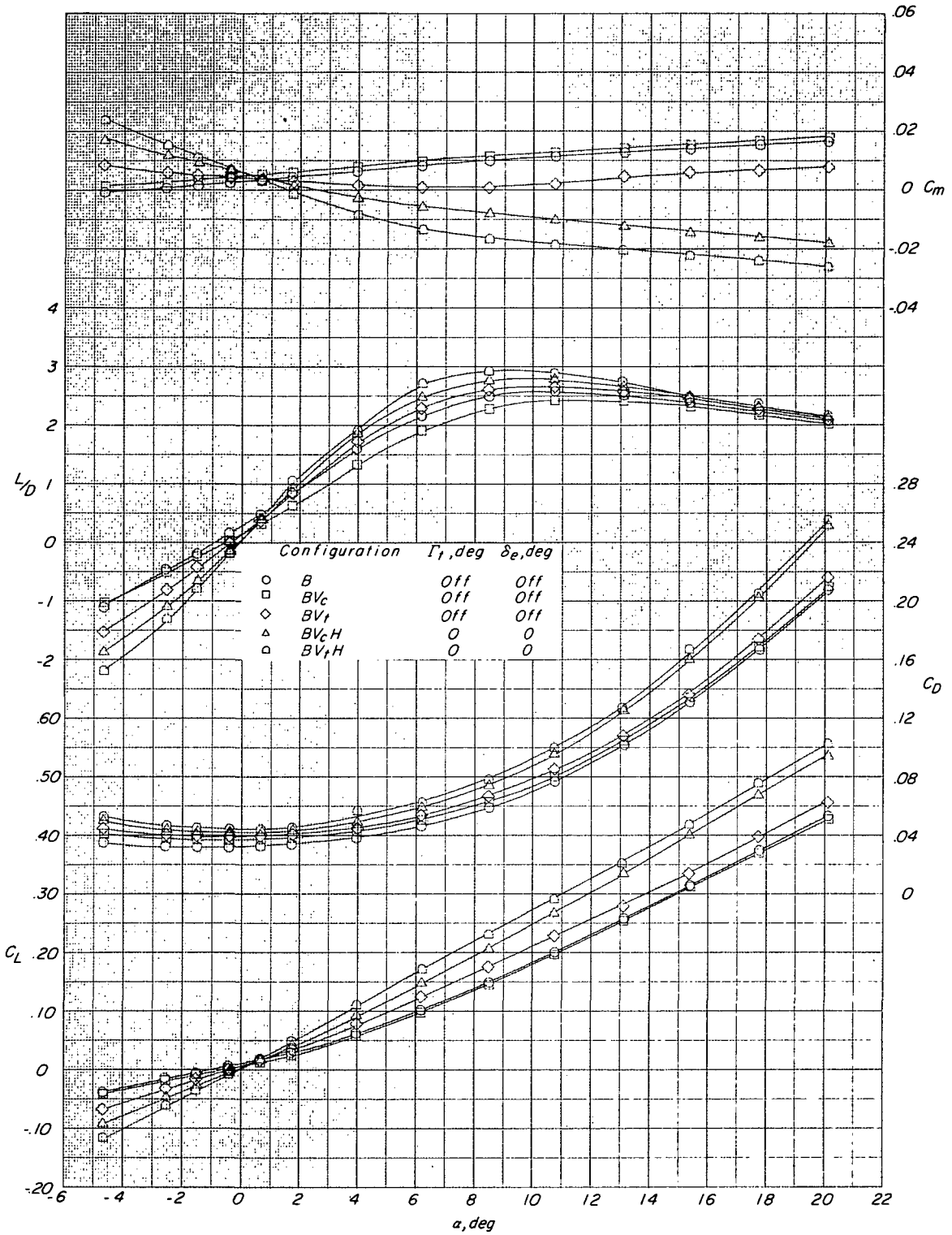

(a) M = 2.30.

Figure 4.- Longitudinal aerodynamic characteristics of the various configurations.

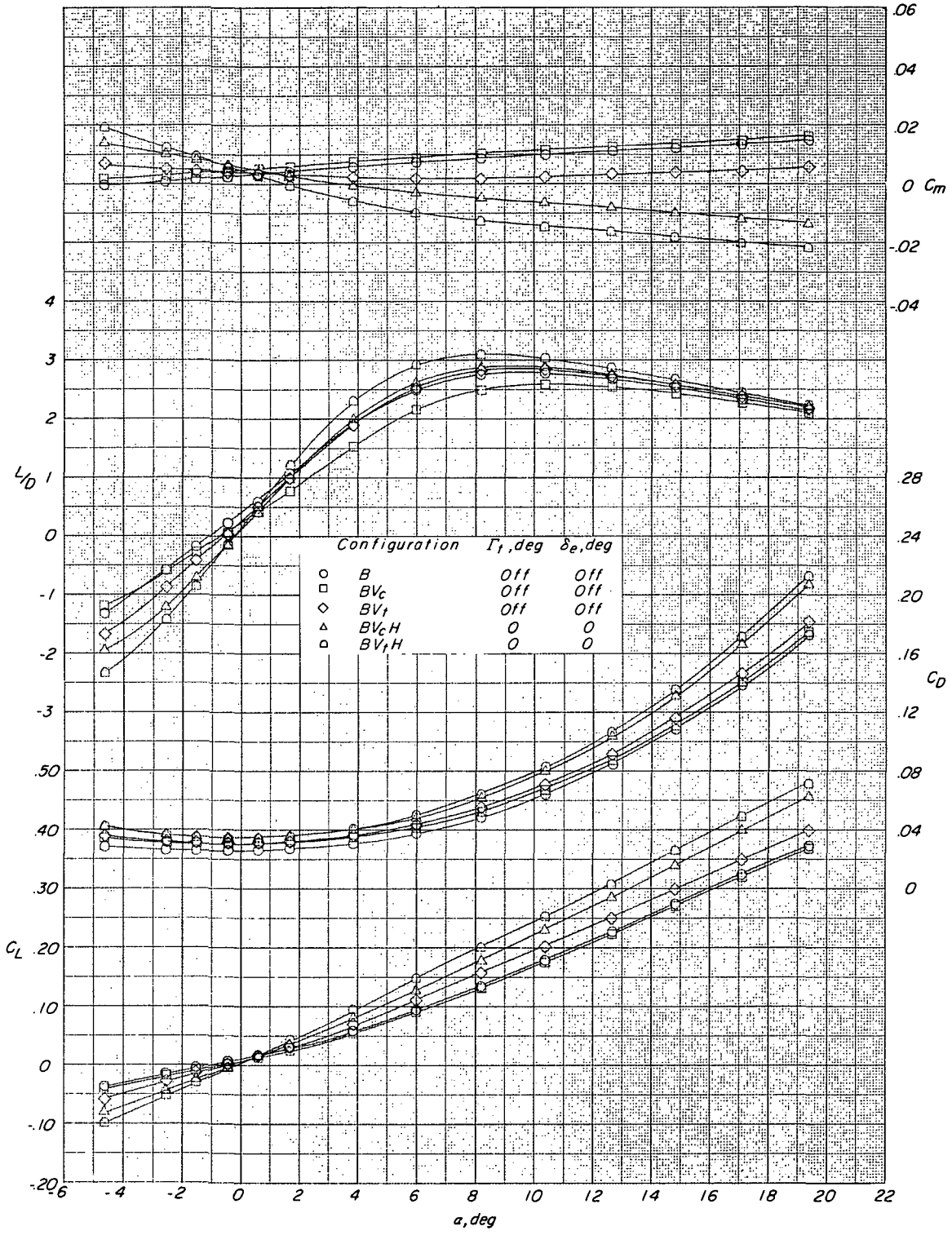

(b) M = 2.96.

Figure 4.- Continued.

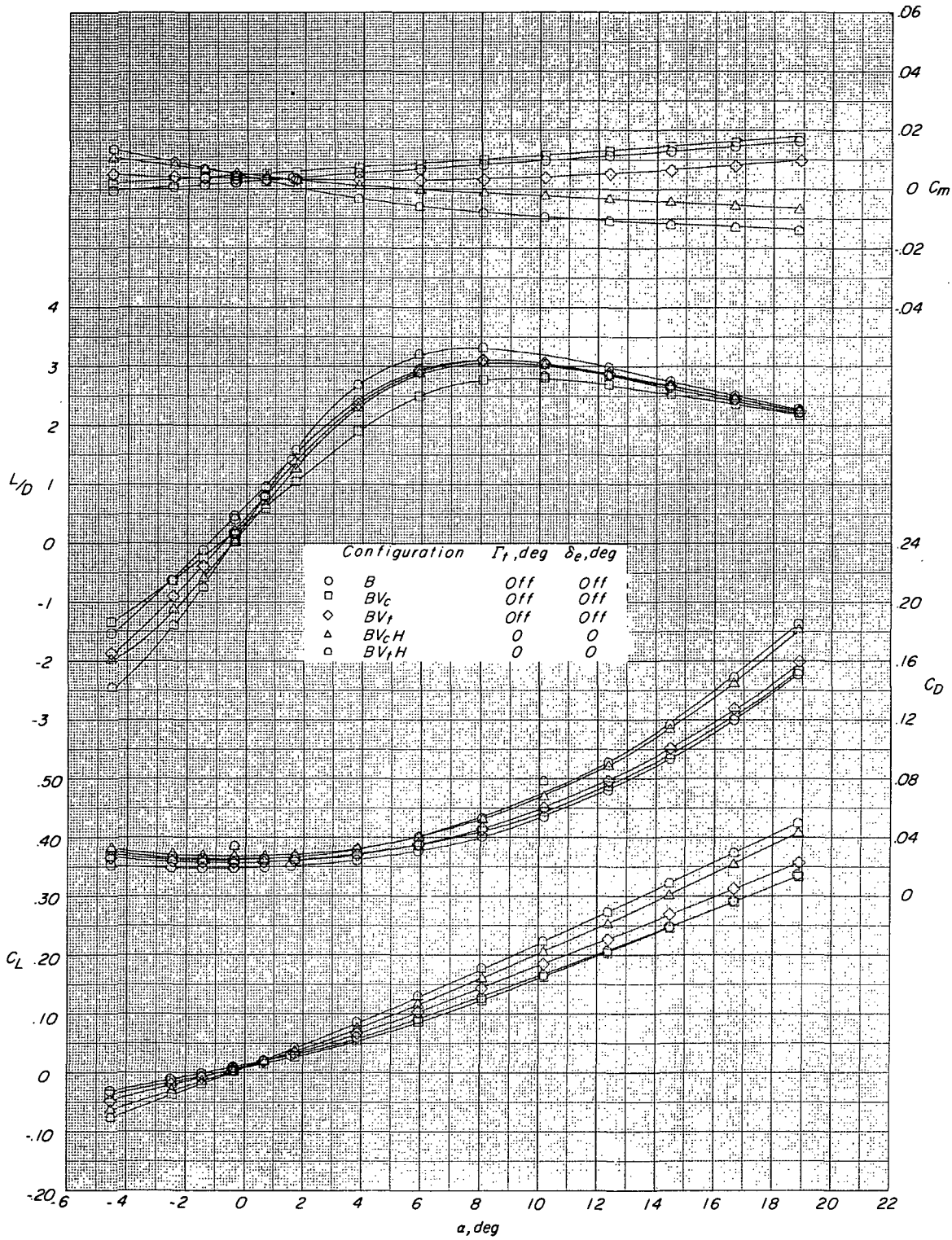

(c) M = 3.96.

Figure 4.- Continued.

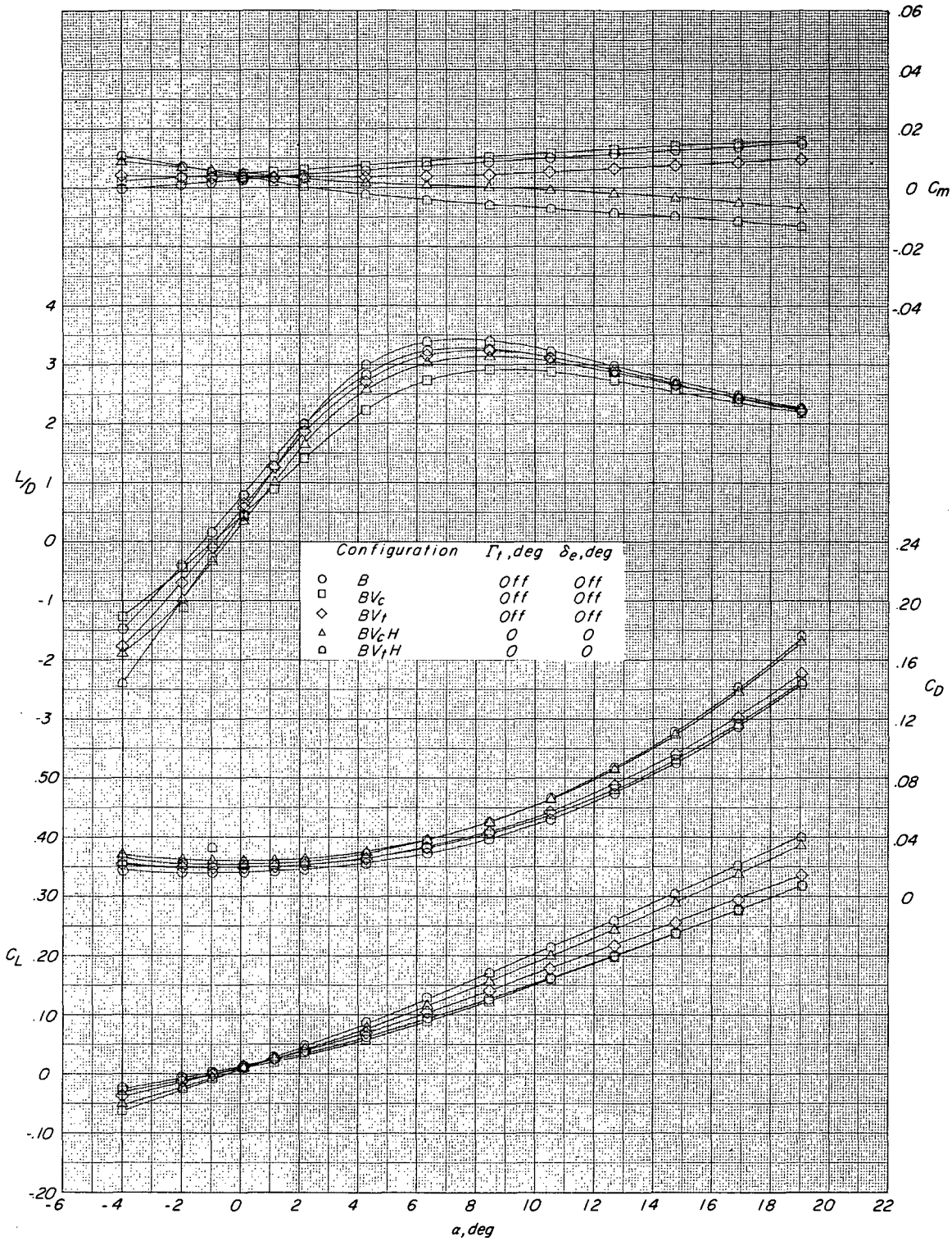

(d) M = 4.63.

Figure 4.- Concluded.

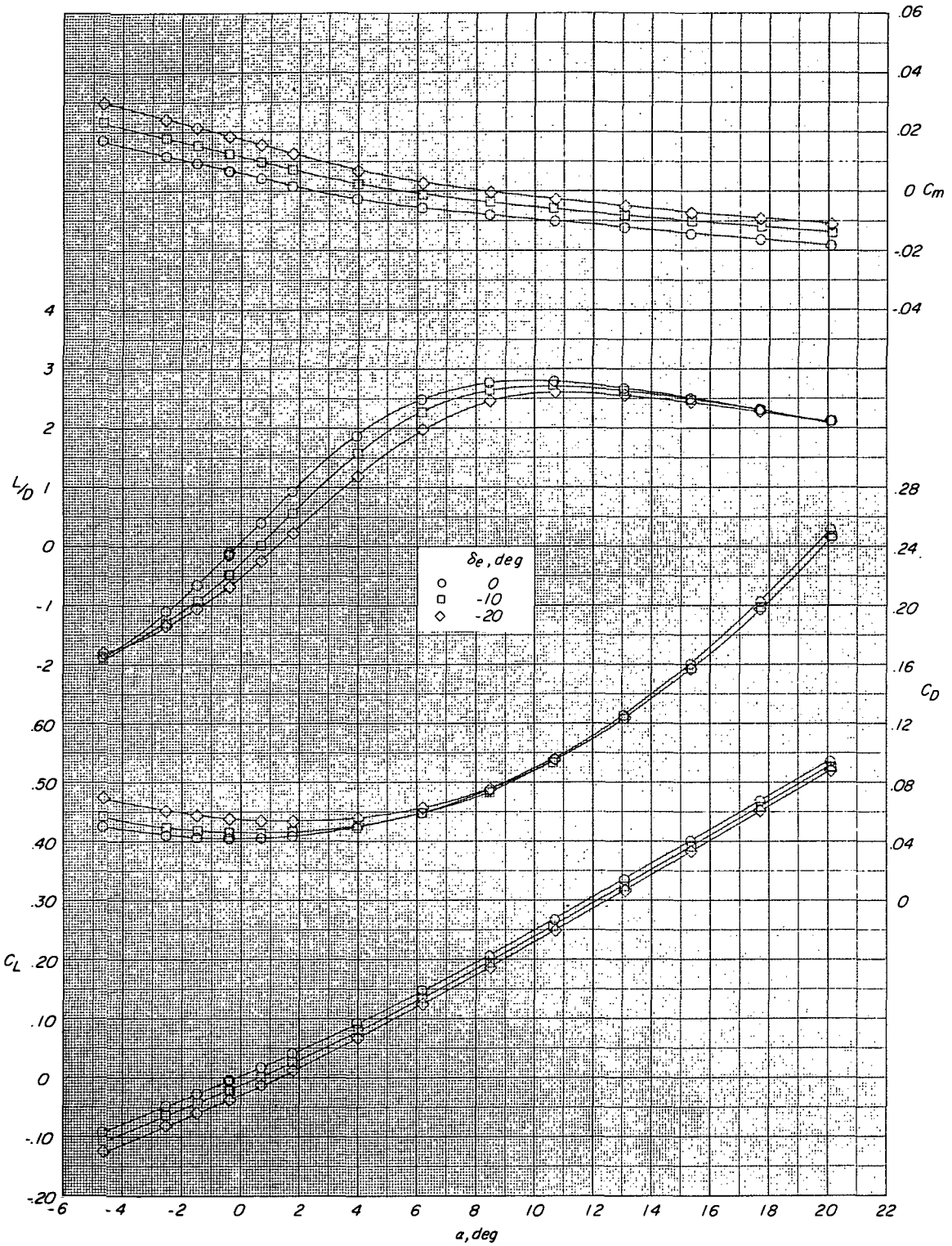

(a) M = 2.30.

Figure 5.- Longitudinal control characteristics for the configuration BV_cH having $\Gamma_t = 0^o$ and $\Gamma_v = 90^o$.

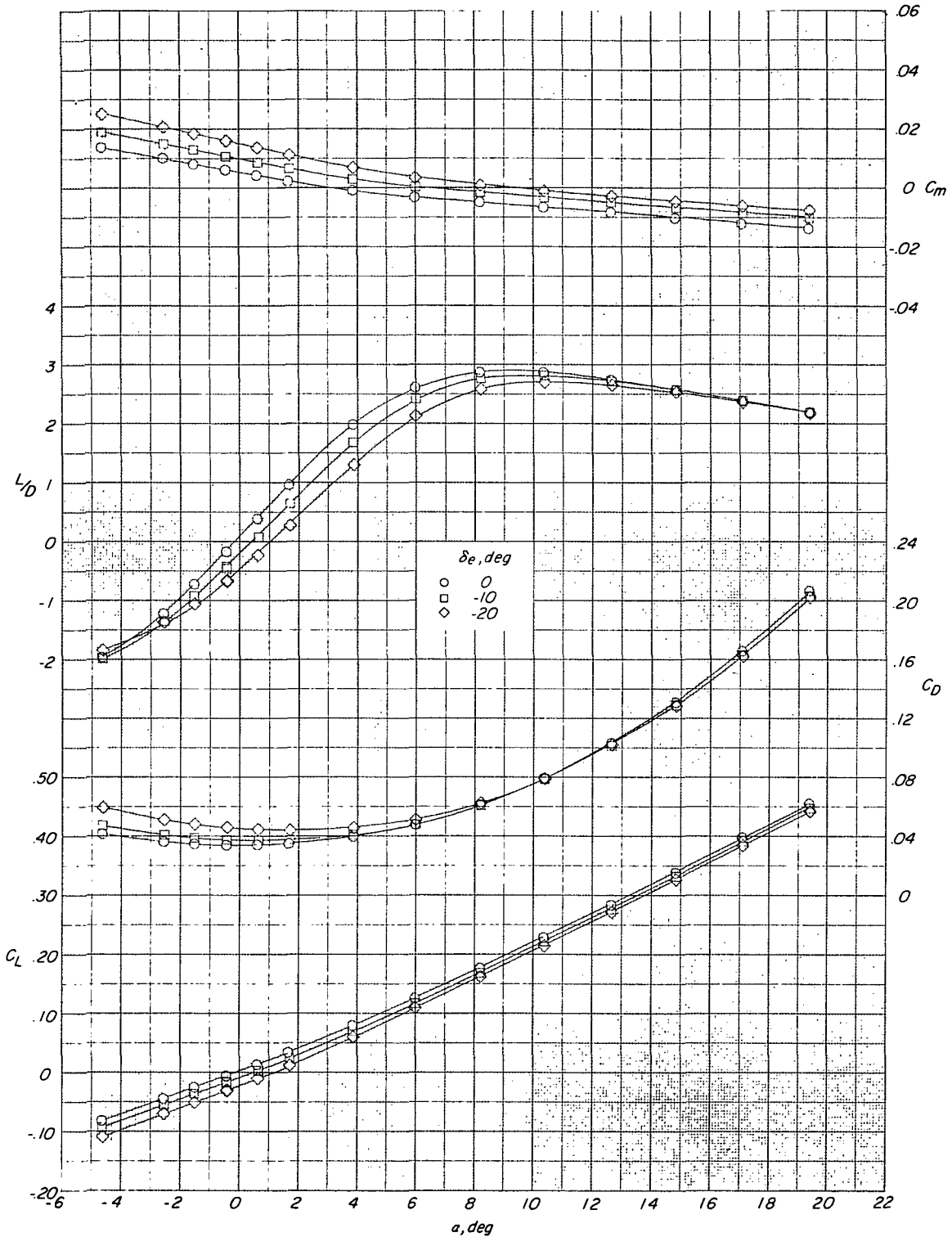

(b) M = 2.96.

Figure 5.- Continued.

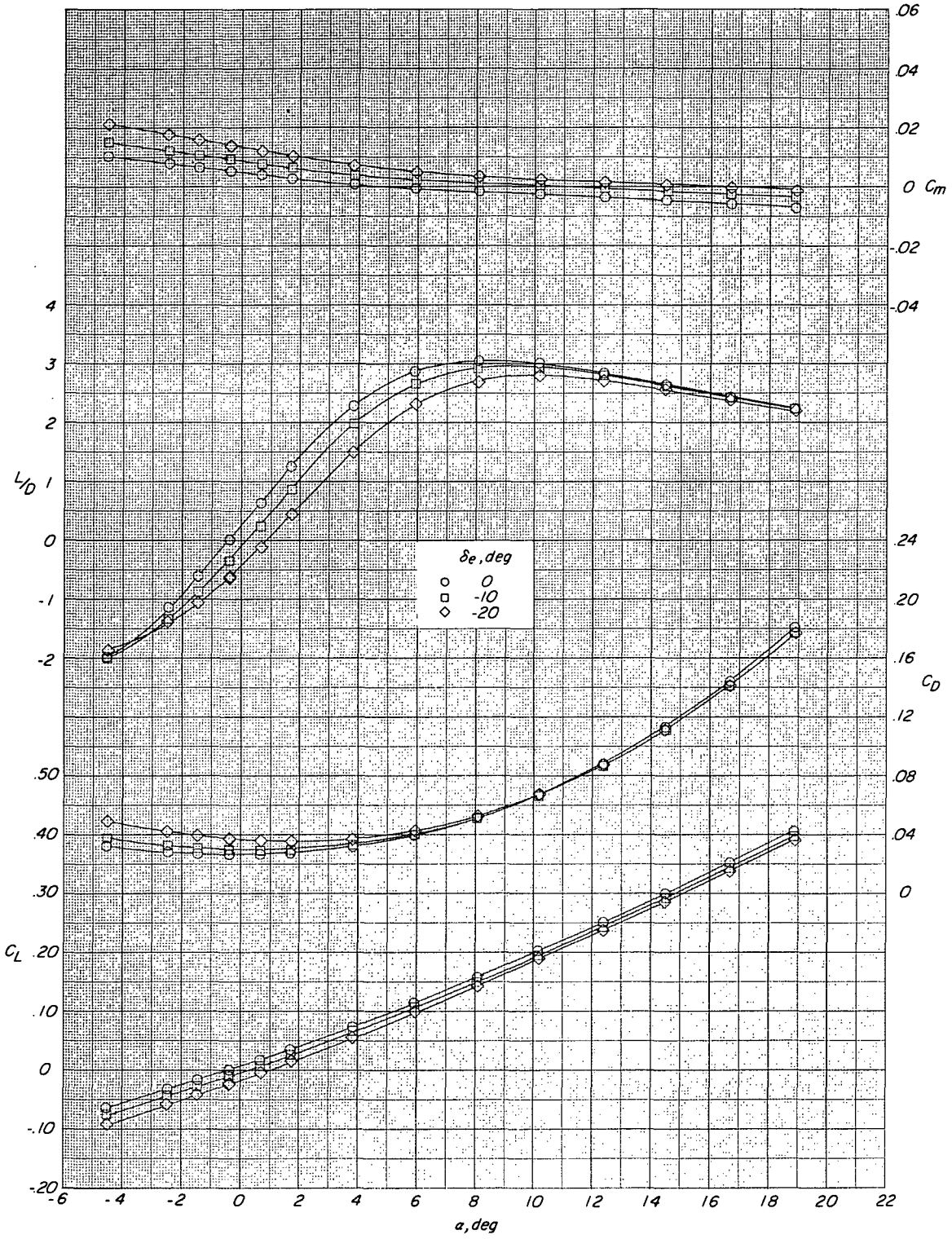

(c) M = 3.96.

Figure 5.- Continued.

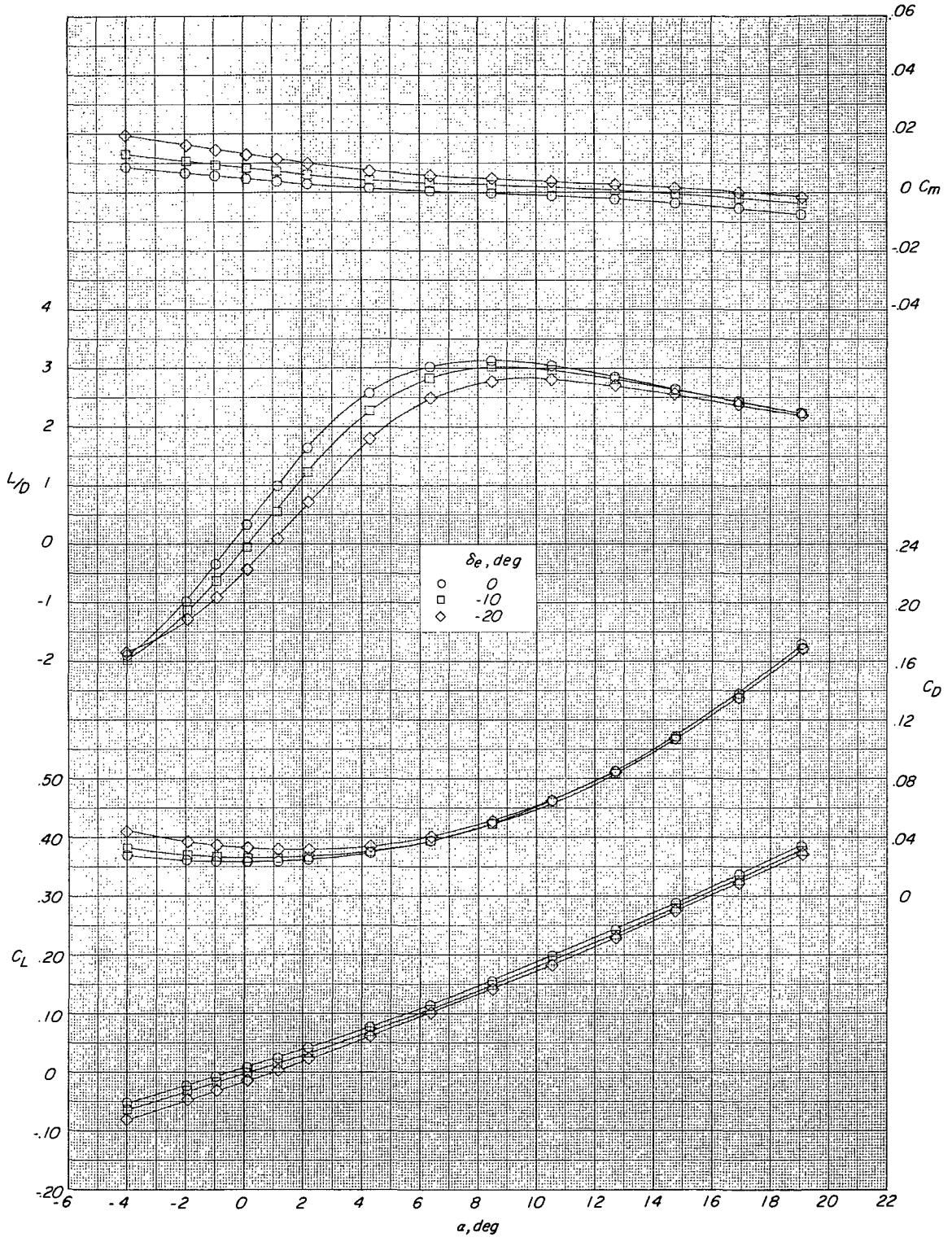

(d) M = 4.63.

Figure 5.- Concluded.

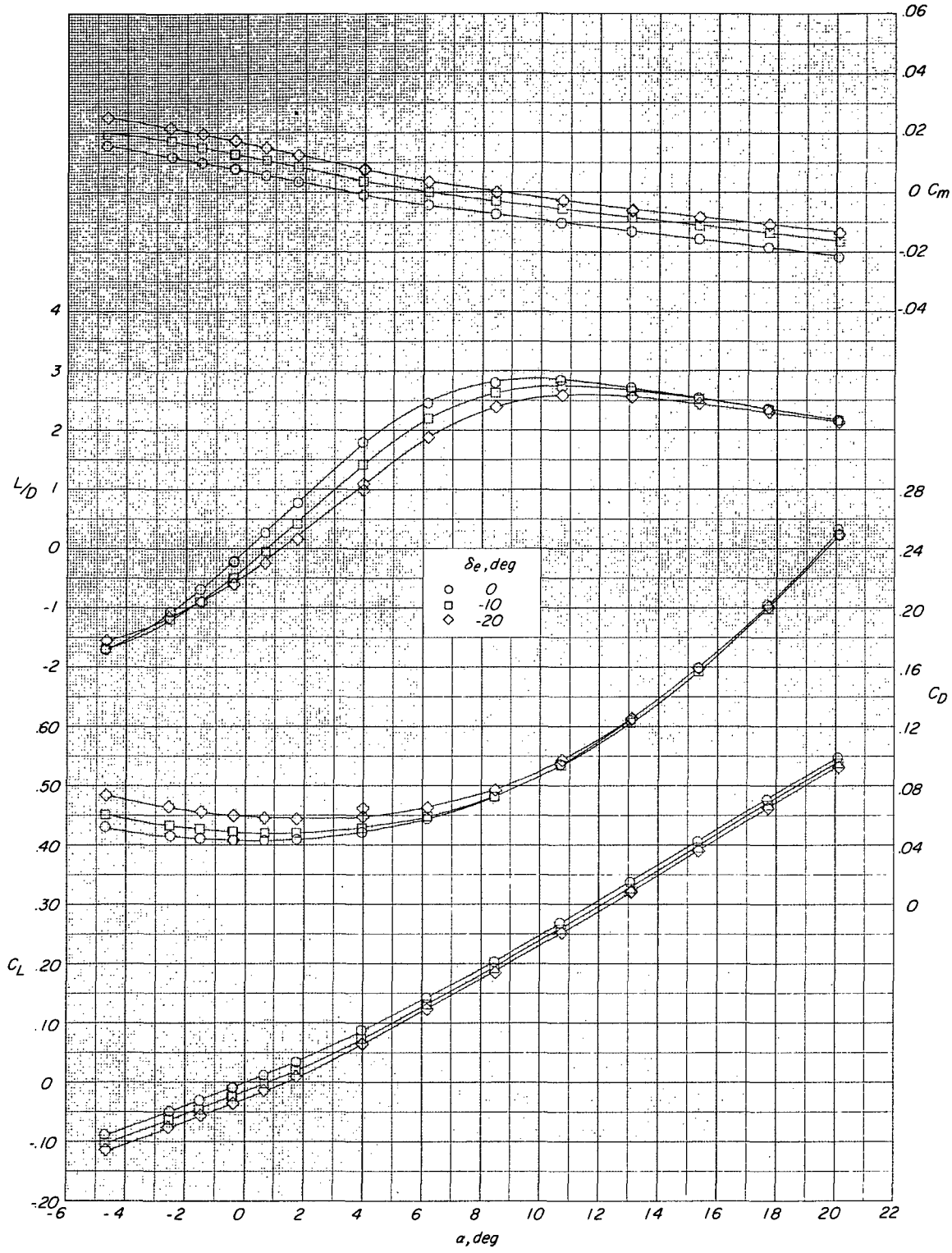

(a) M = 2.30.

Figure 6.- Longitudinal control characteristics for the configuration BV_cH having $\Gamma_t = -30^o$ and $\Gamma_v = 90^o$.

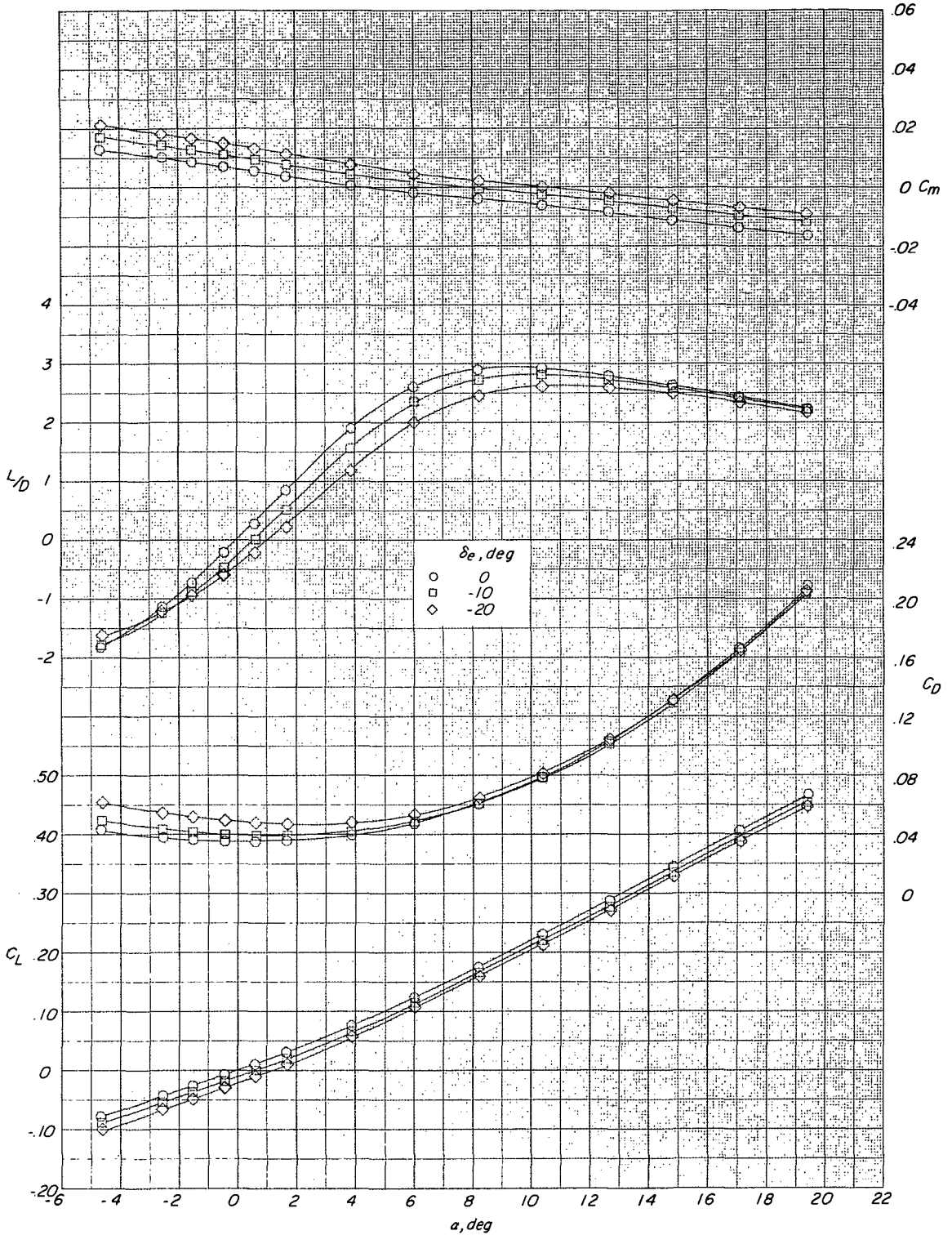

(b) M = 2.96.

Figure 6.- Continued.

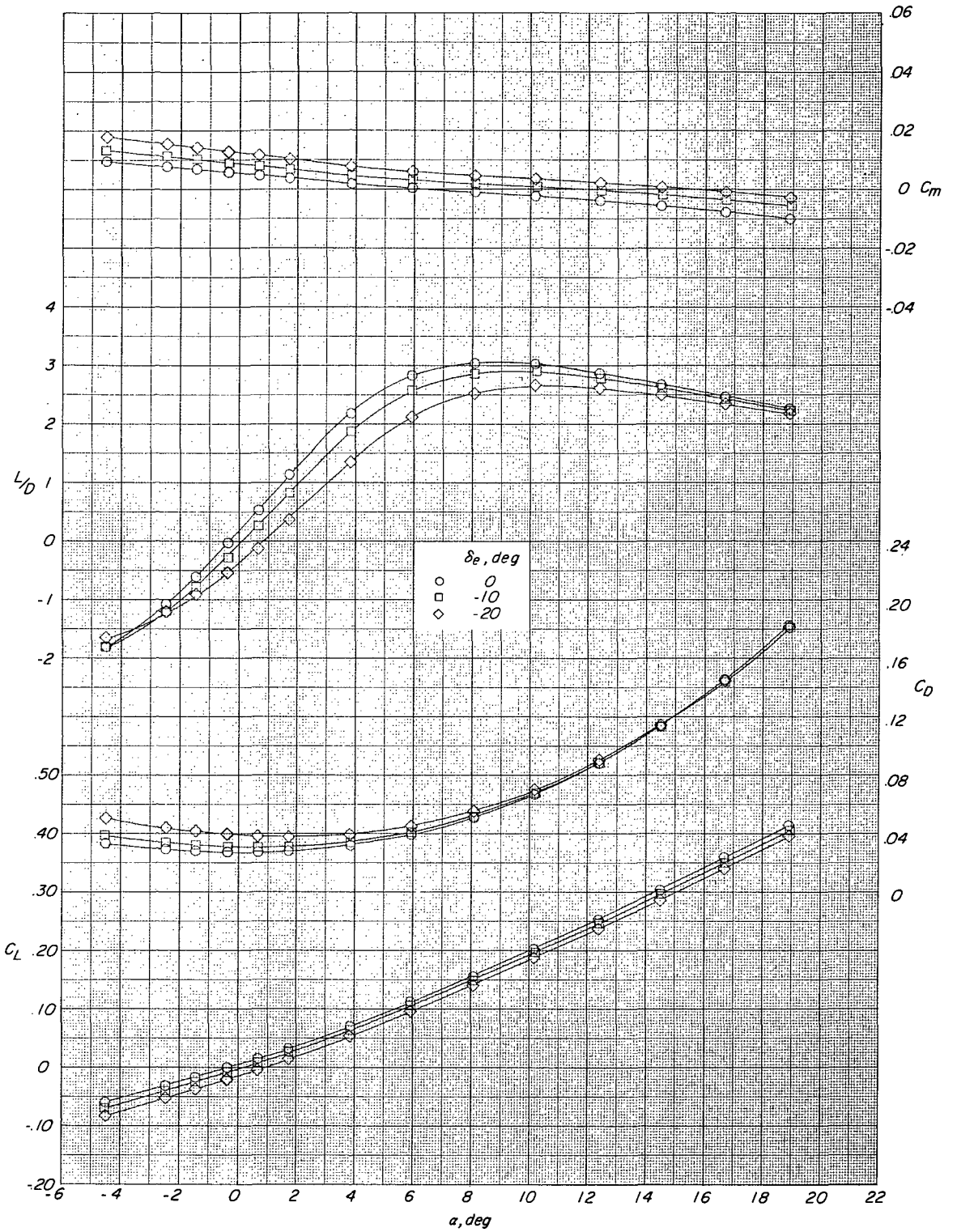

(c) M = 3.96.

Figure 6.- Continued.

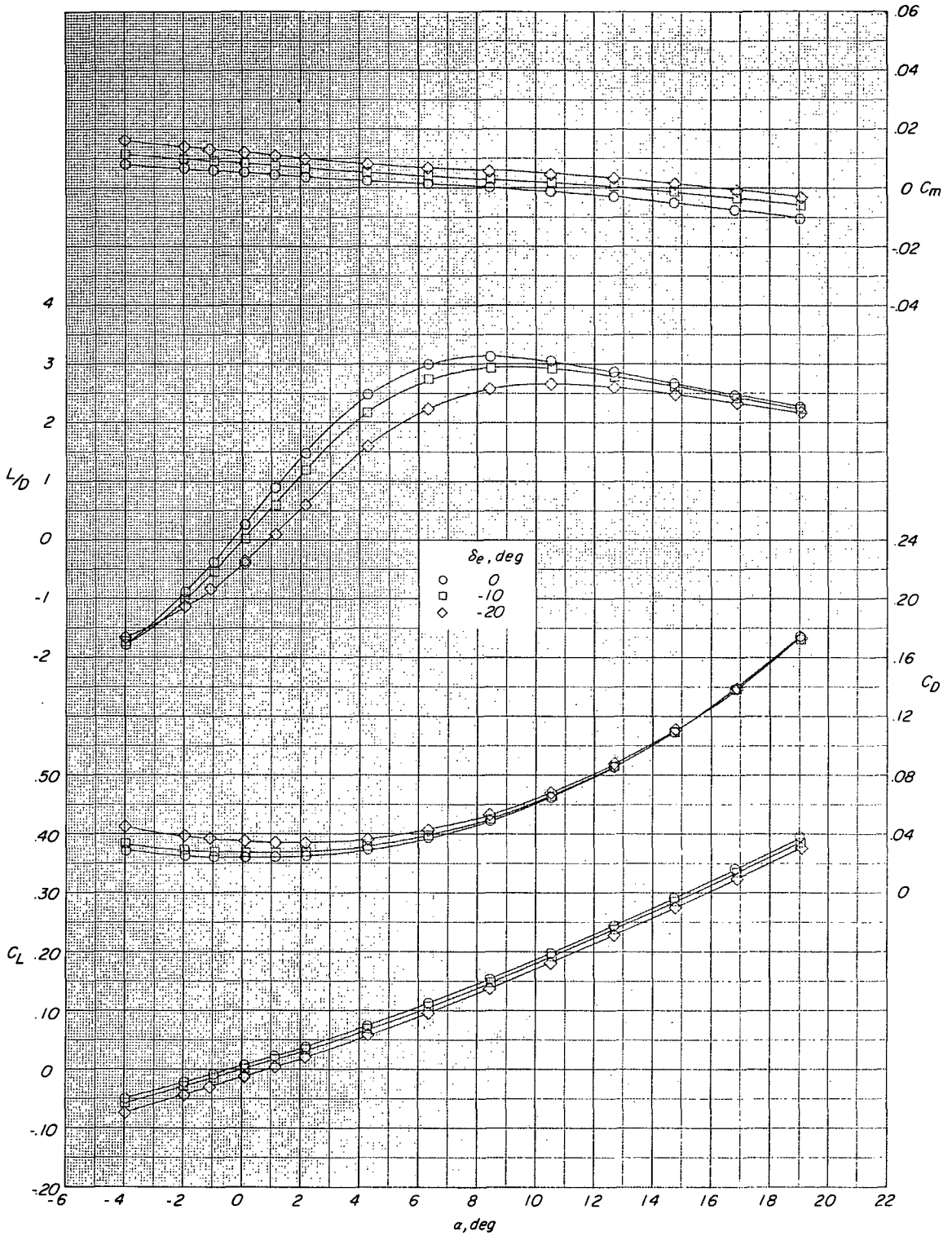

(d) M = 4.63.

Figure 6.- Concluded.

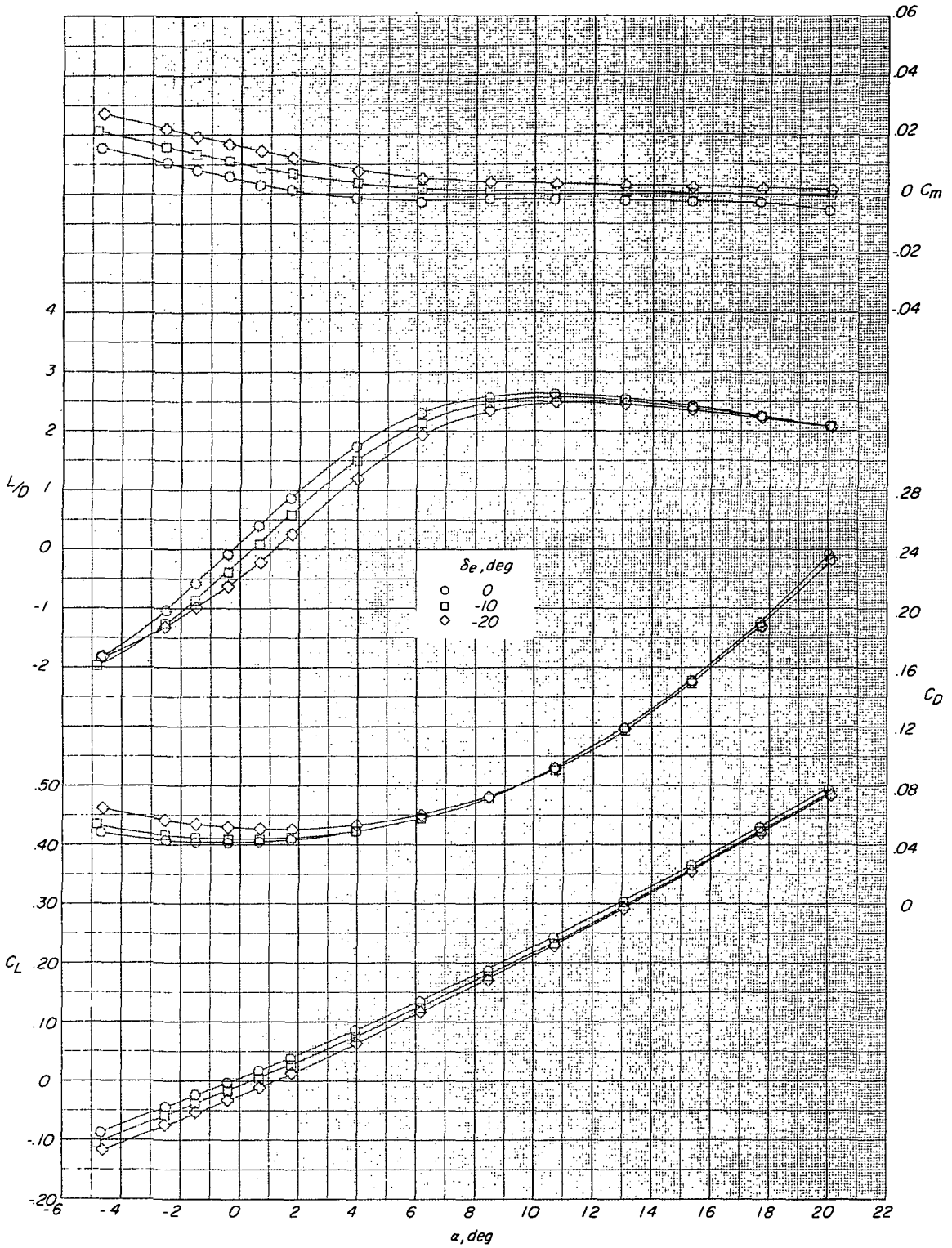

(a) M = 2.30.

Figure 7.- Longitudinal control characteristics for the configuration BV_cH having $\Gamma_t = 30^o$ and $\Gamma_v = 90^o$.

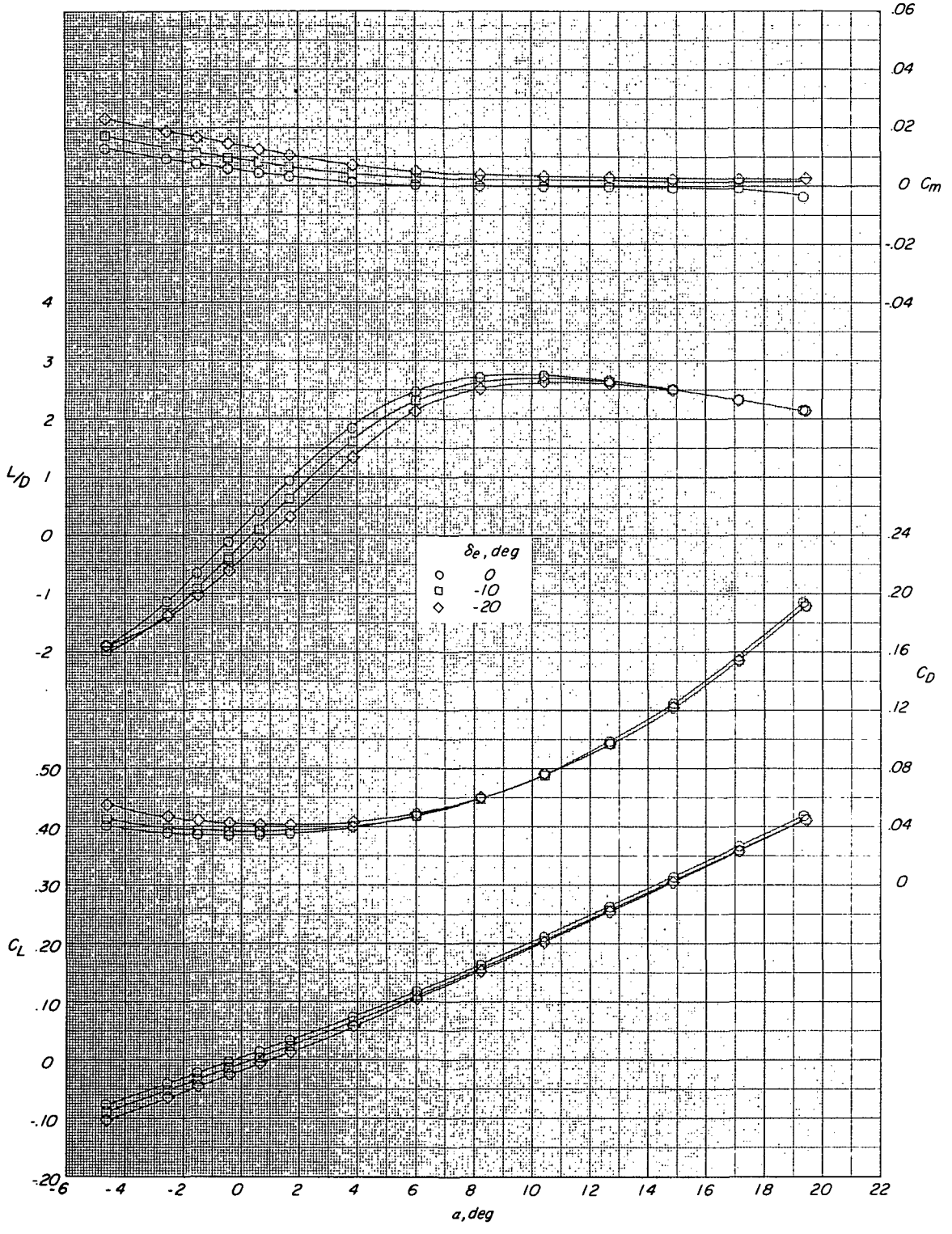

(b) M = 2.96.

Figure 7.- Continued.

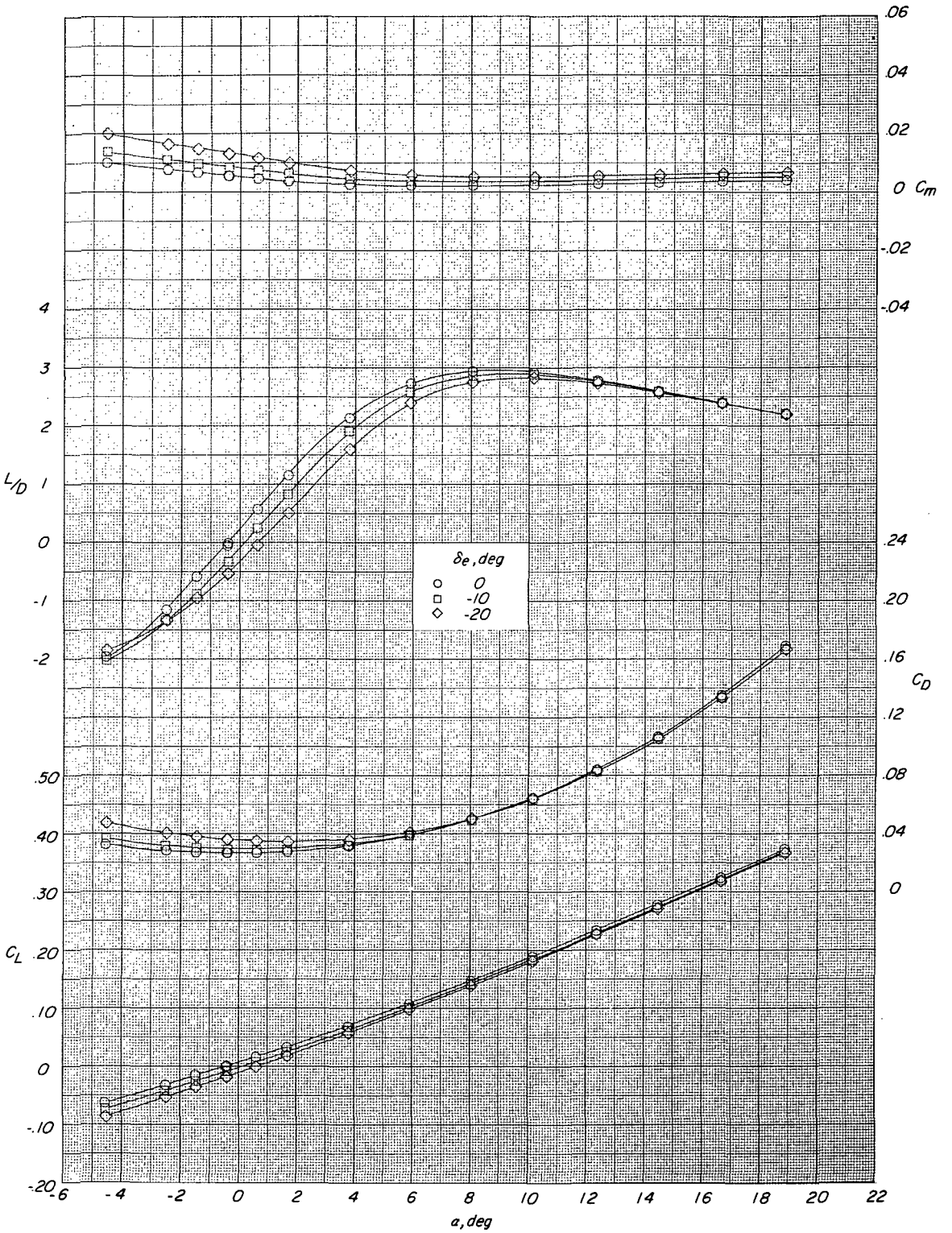

(c) M = 3.96.

Figure 7.- Continued.

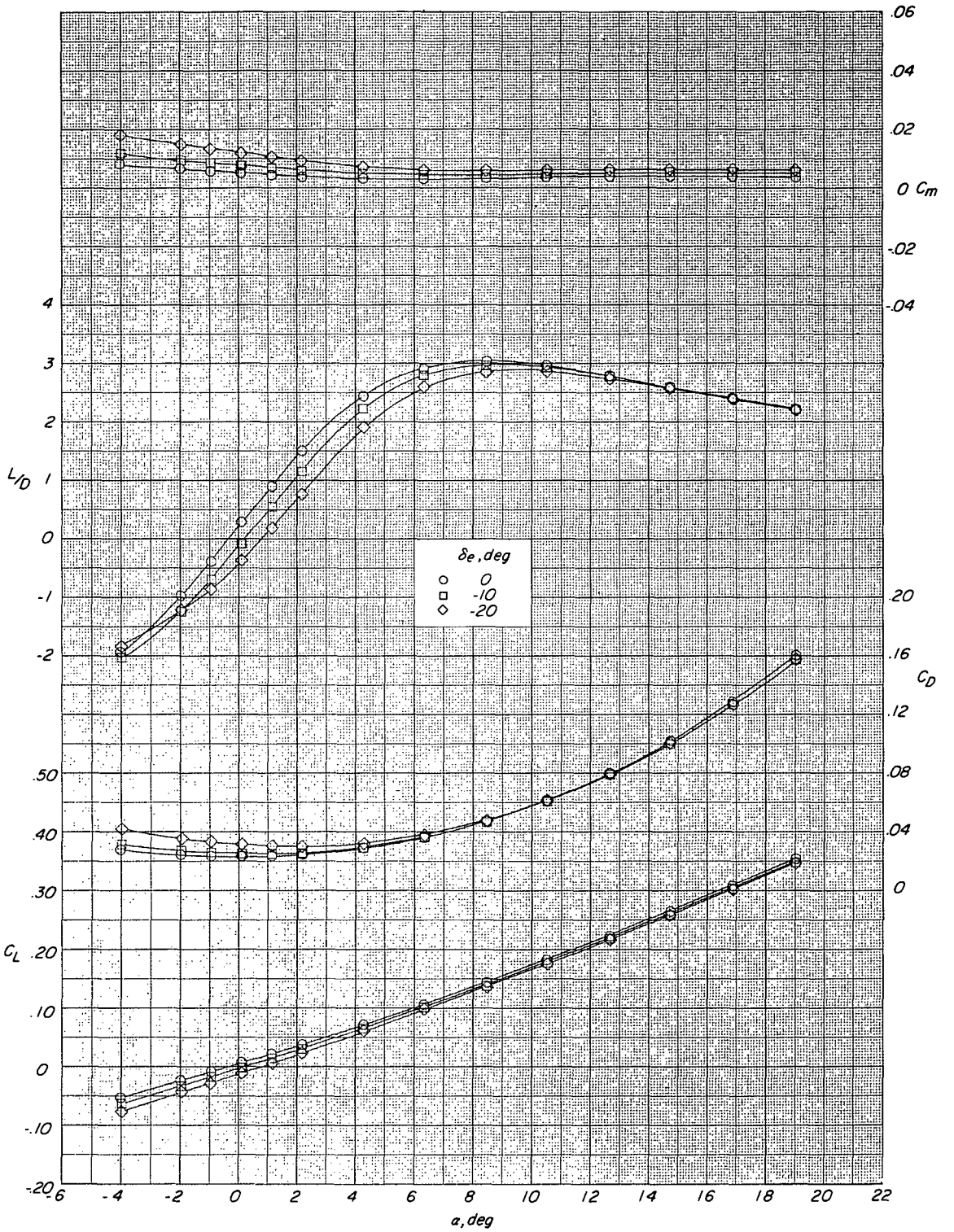

(d) M = 4.63.

Figure 7.- Concluded.

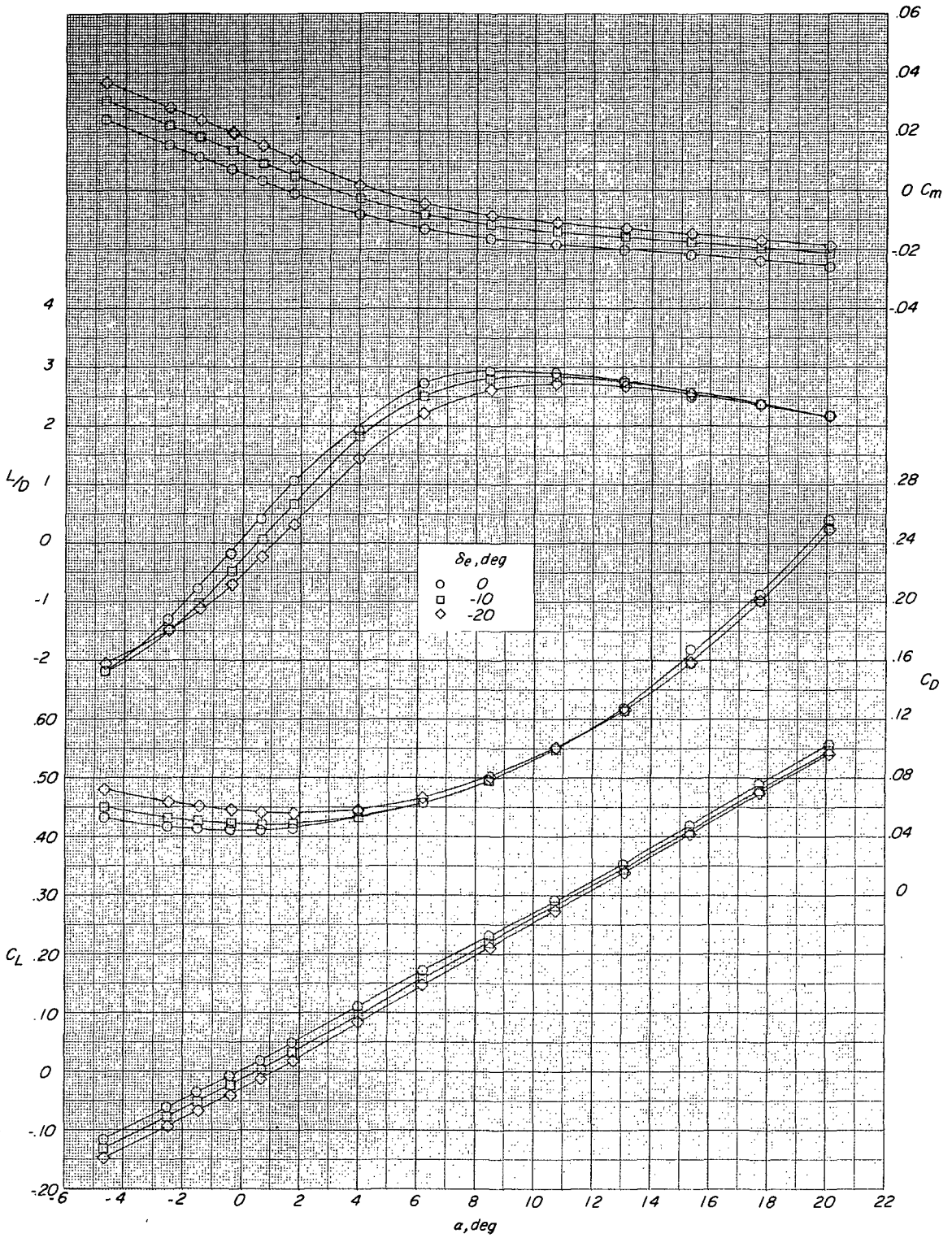

(a) M = 2.30.

Figure 8.- Longitudinal control characteristics for the configuration BV_tH having $\Gamma_t = 0^o$ and $\Gamma_v = 45^o$.

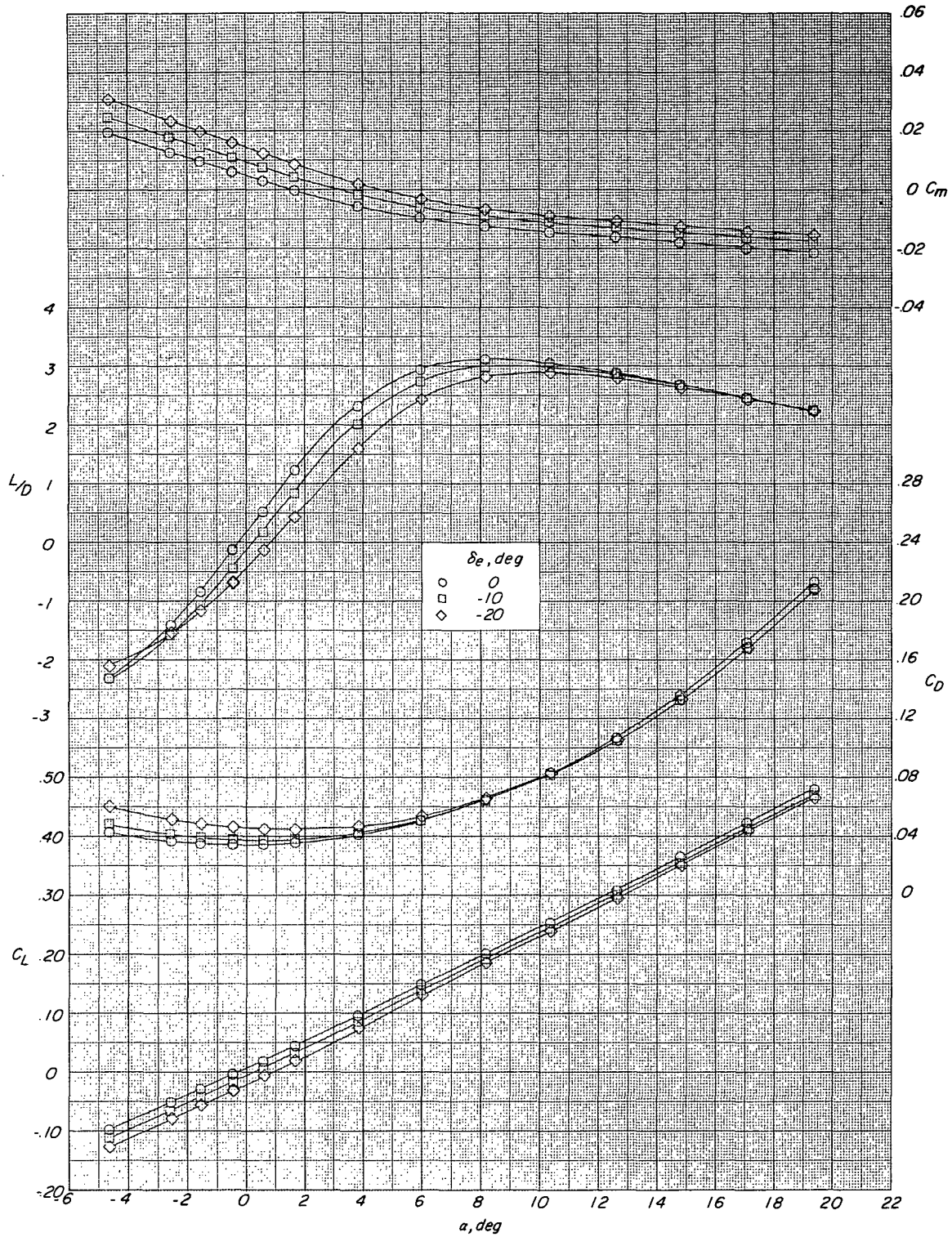

(b) M = 2.96.

Figure 8.- Continued.

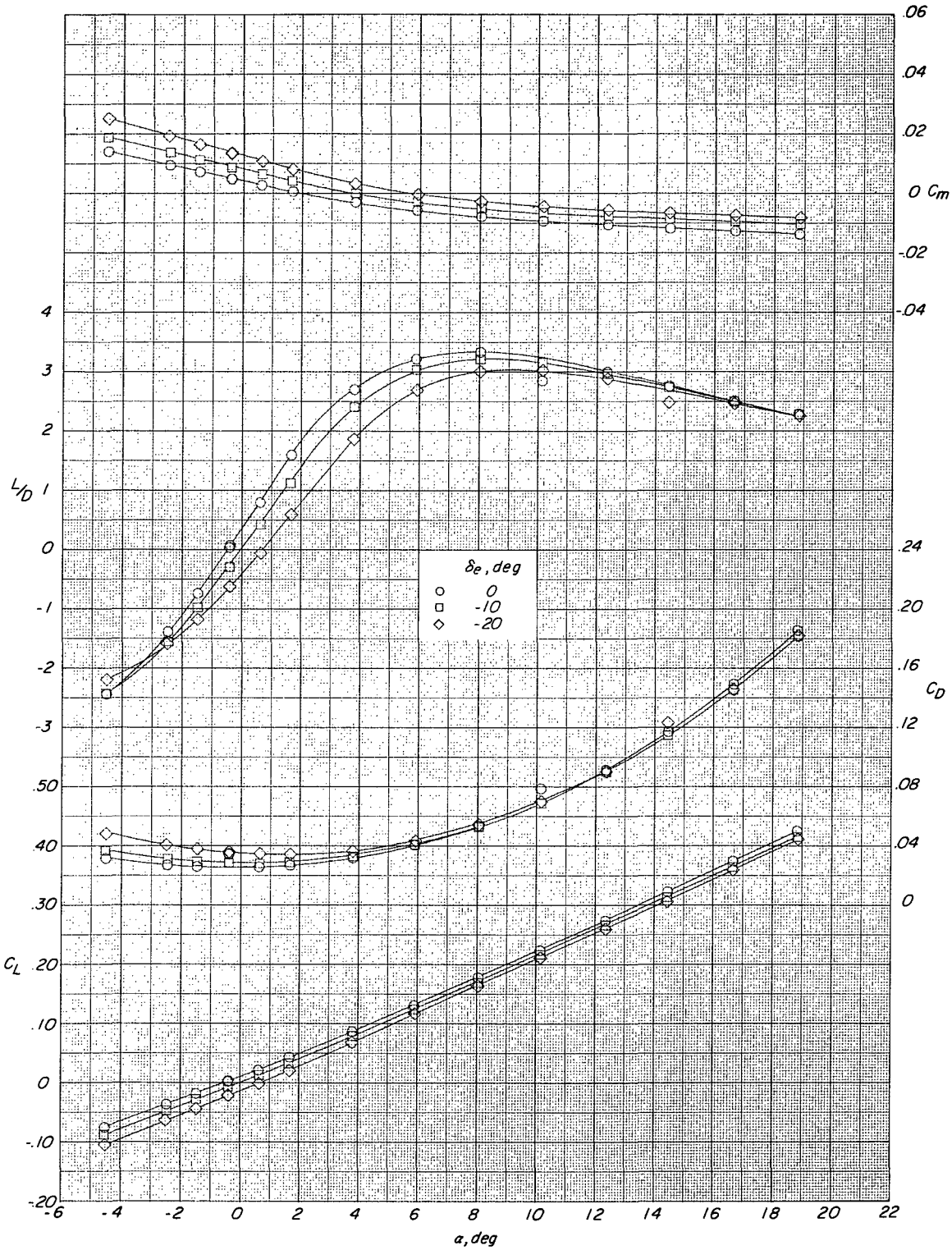

(c) M = 3.96.

Figure 8.- Continued.

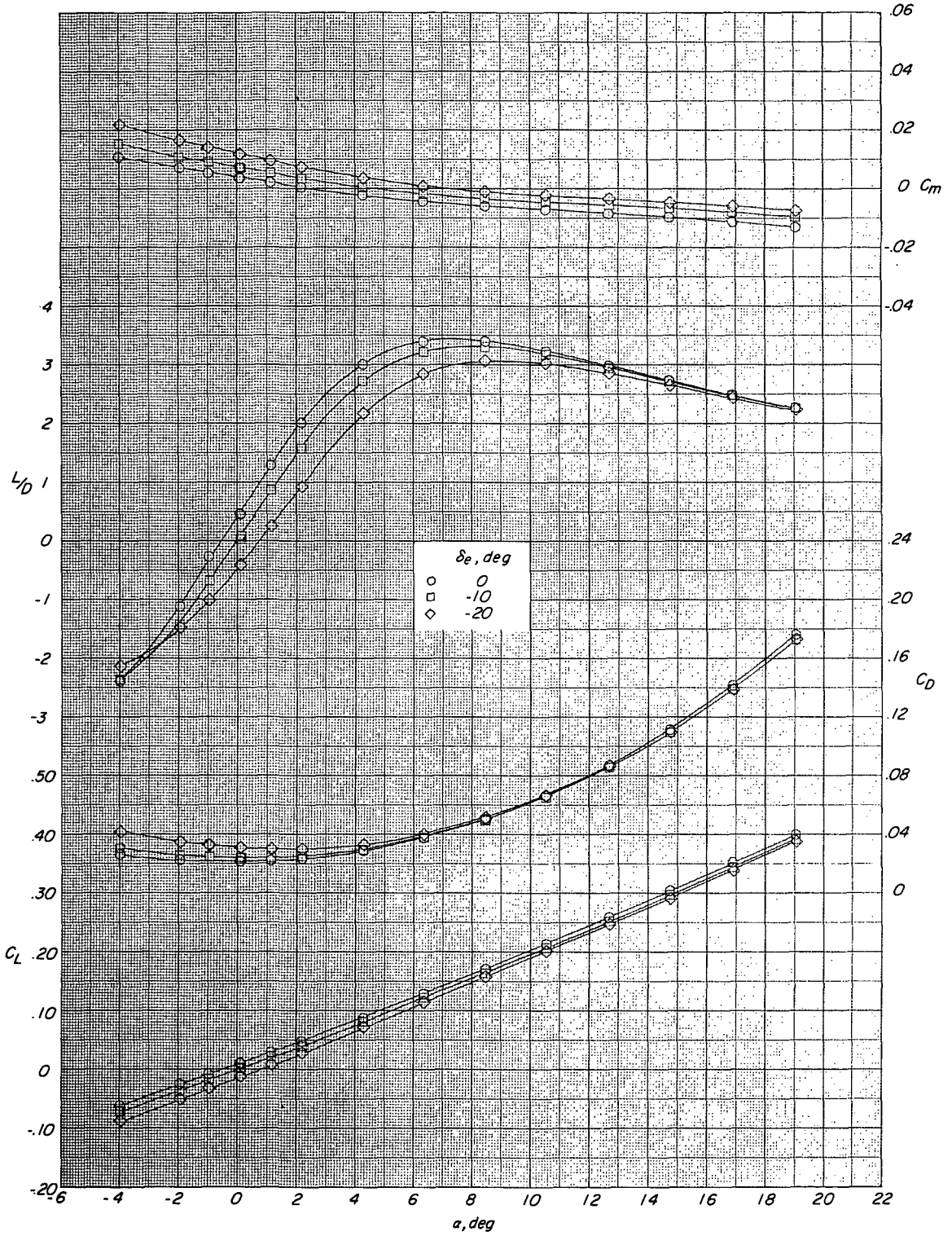

(d) M = 4.63.

Figure 8.- Concluded.

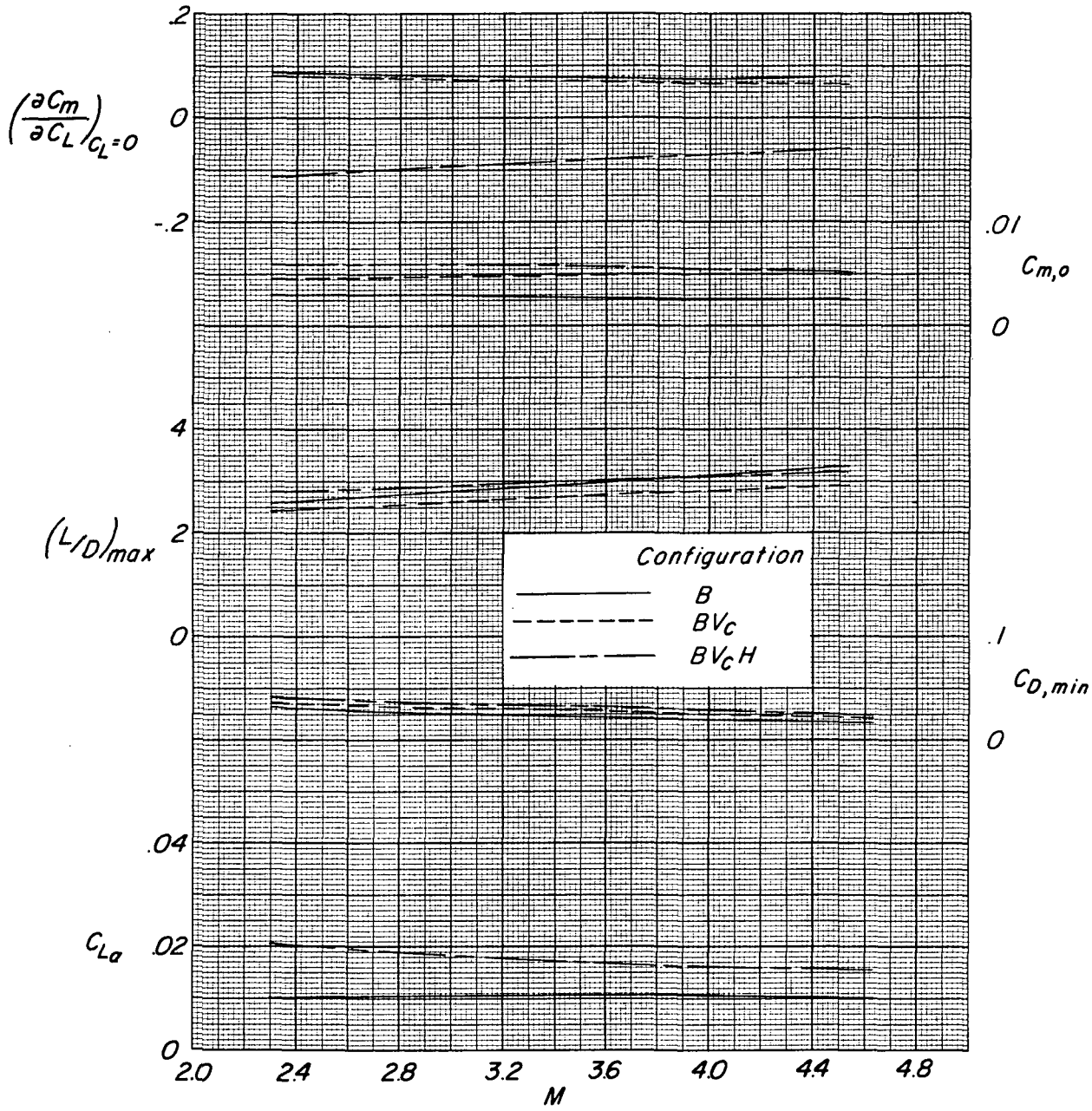

(a) Center-line vertical tail.

Figure 9.- Summary of aerodynamic characteristics.

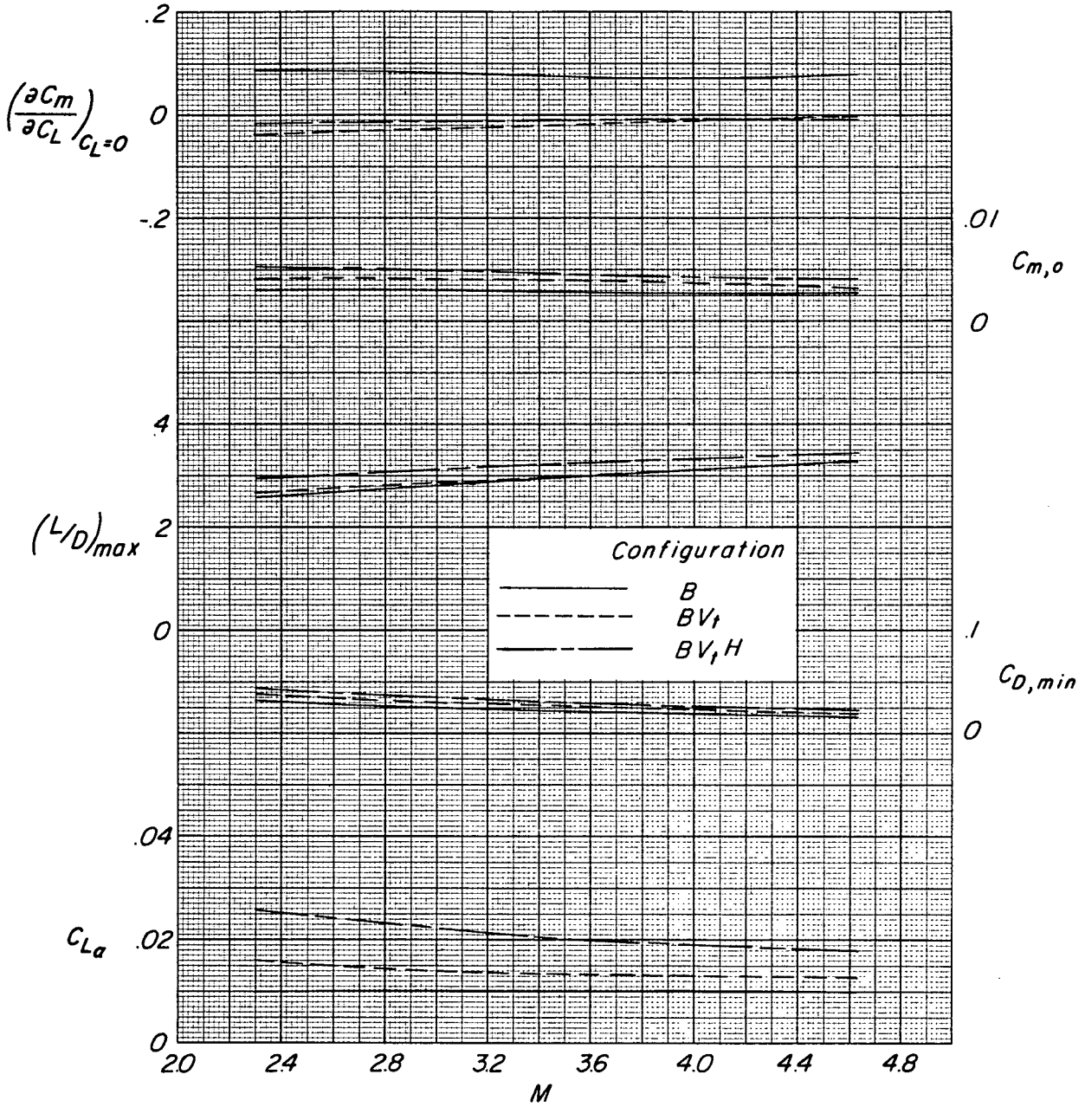

(b) Dorsal fins.

Figure 9.- Concluded.

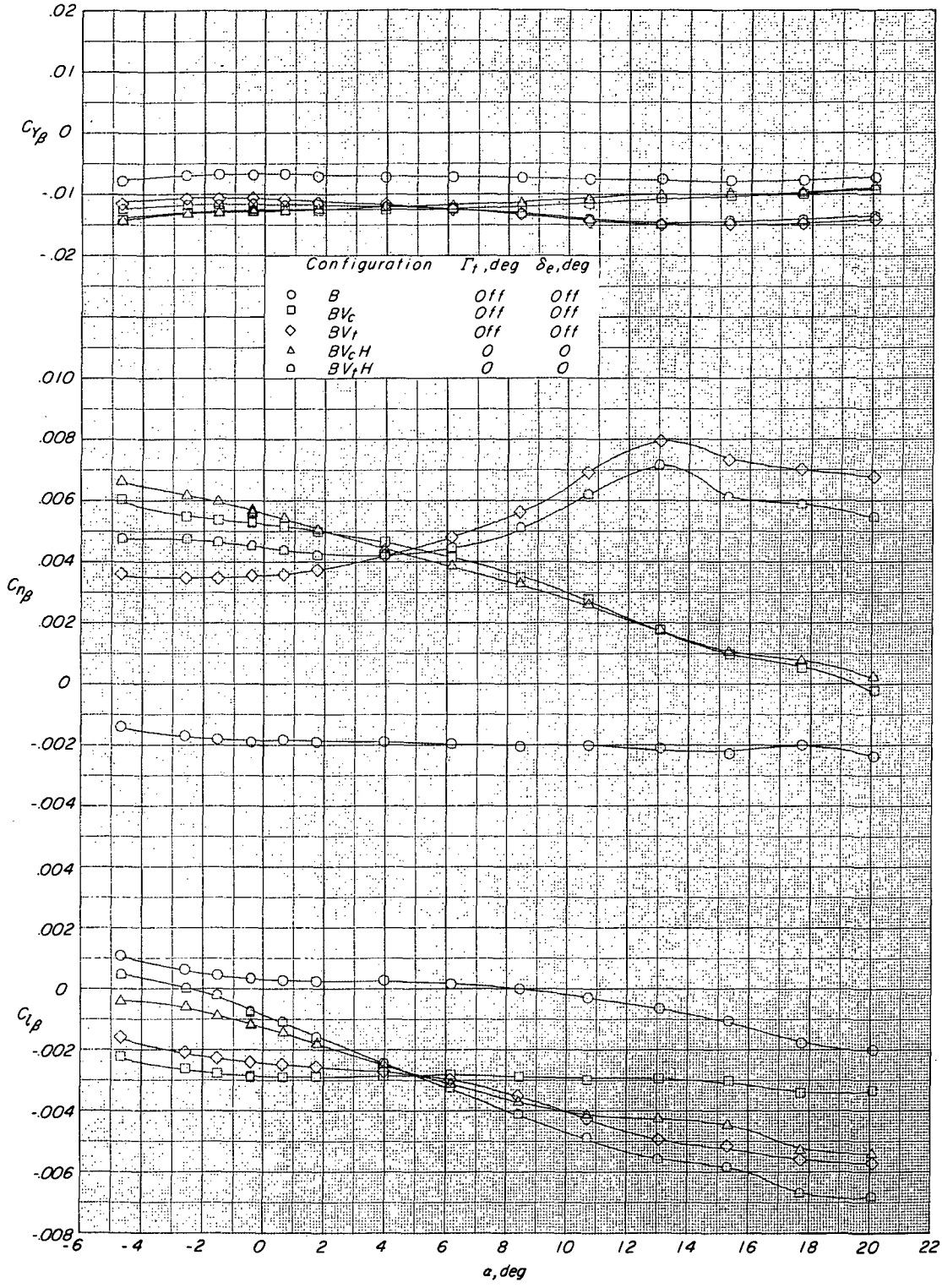

(a) M = 2.30.

Figure 10.- Summary of the lateral-directional stability characteristics for various configurations.

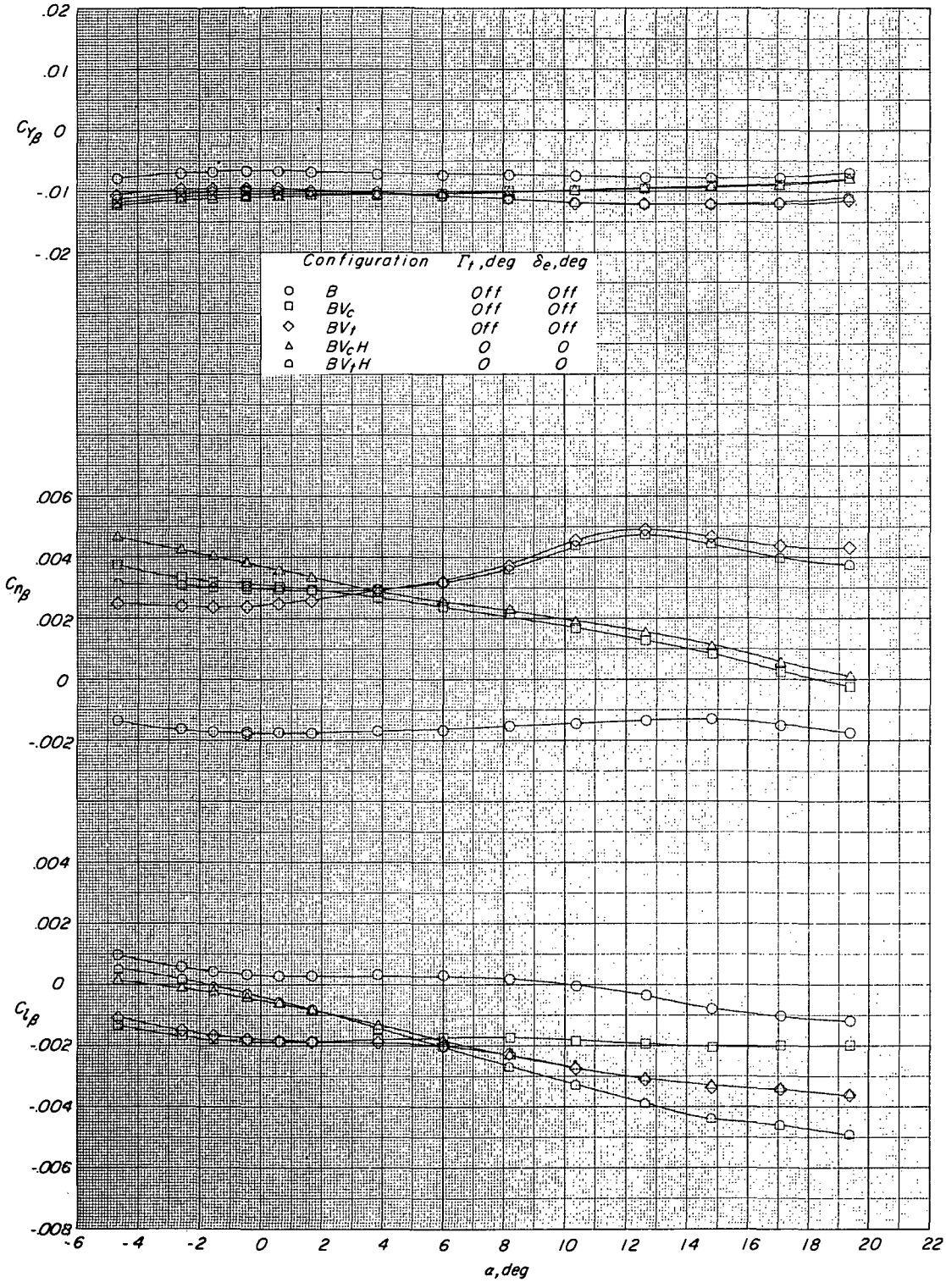

(b) M = 2.96.

Figure 10.- Continued.

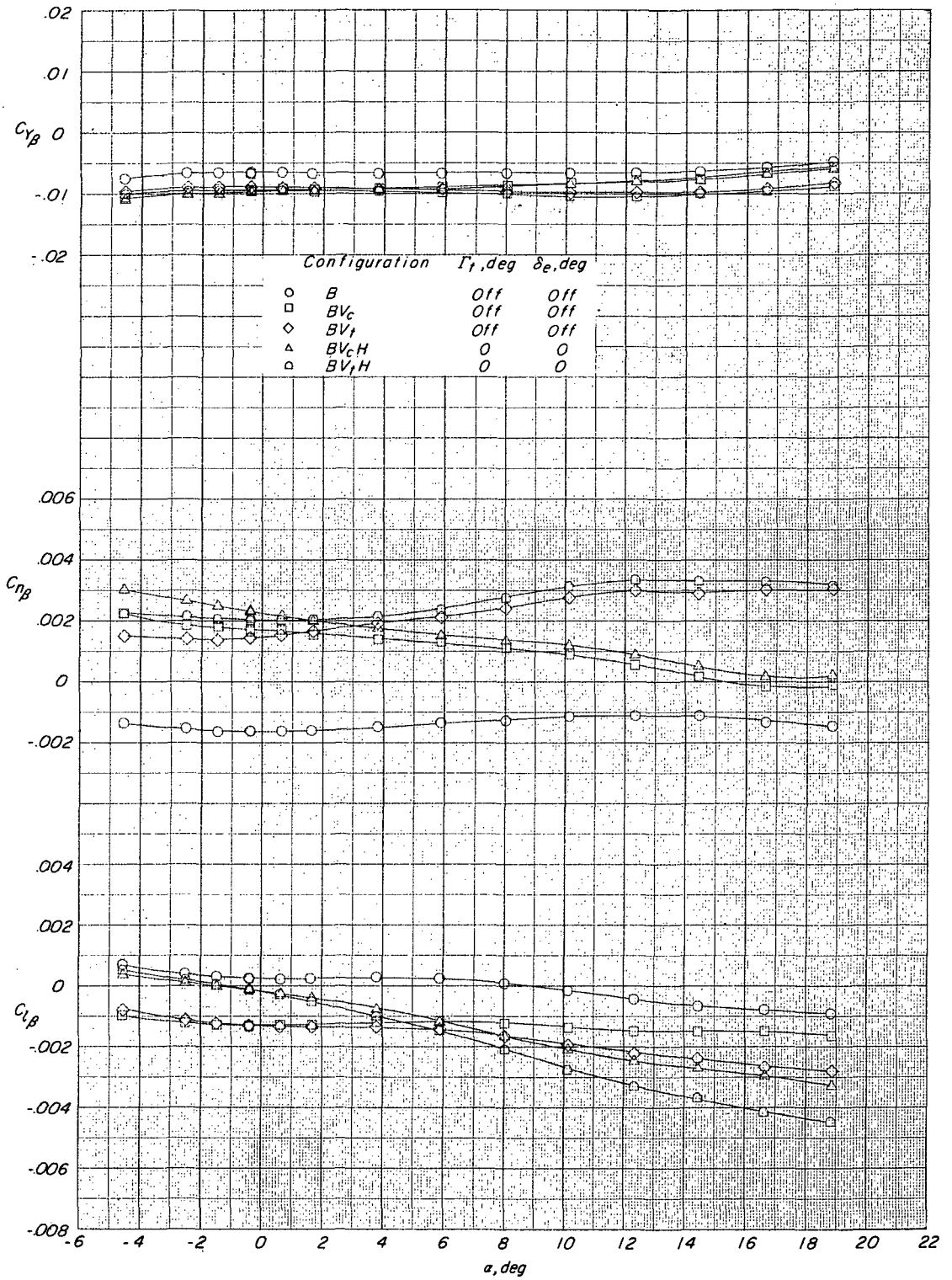

(c) M = 3.96.

Figure 10.- Continued.

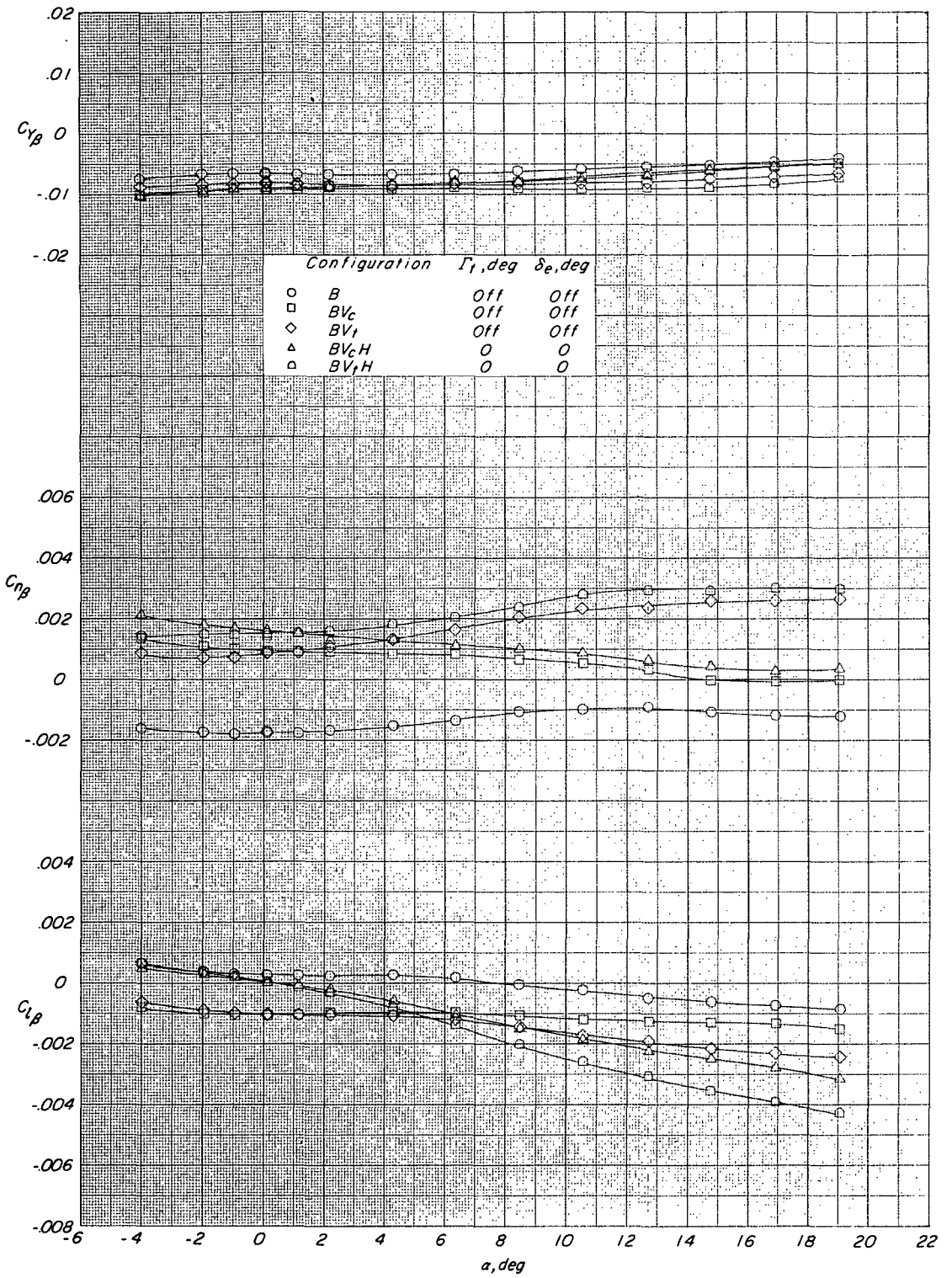

(d) M = 4.63.

Figure 10.- Concluded.

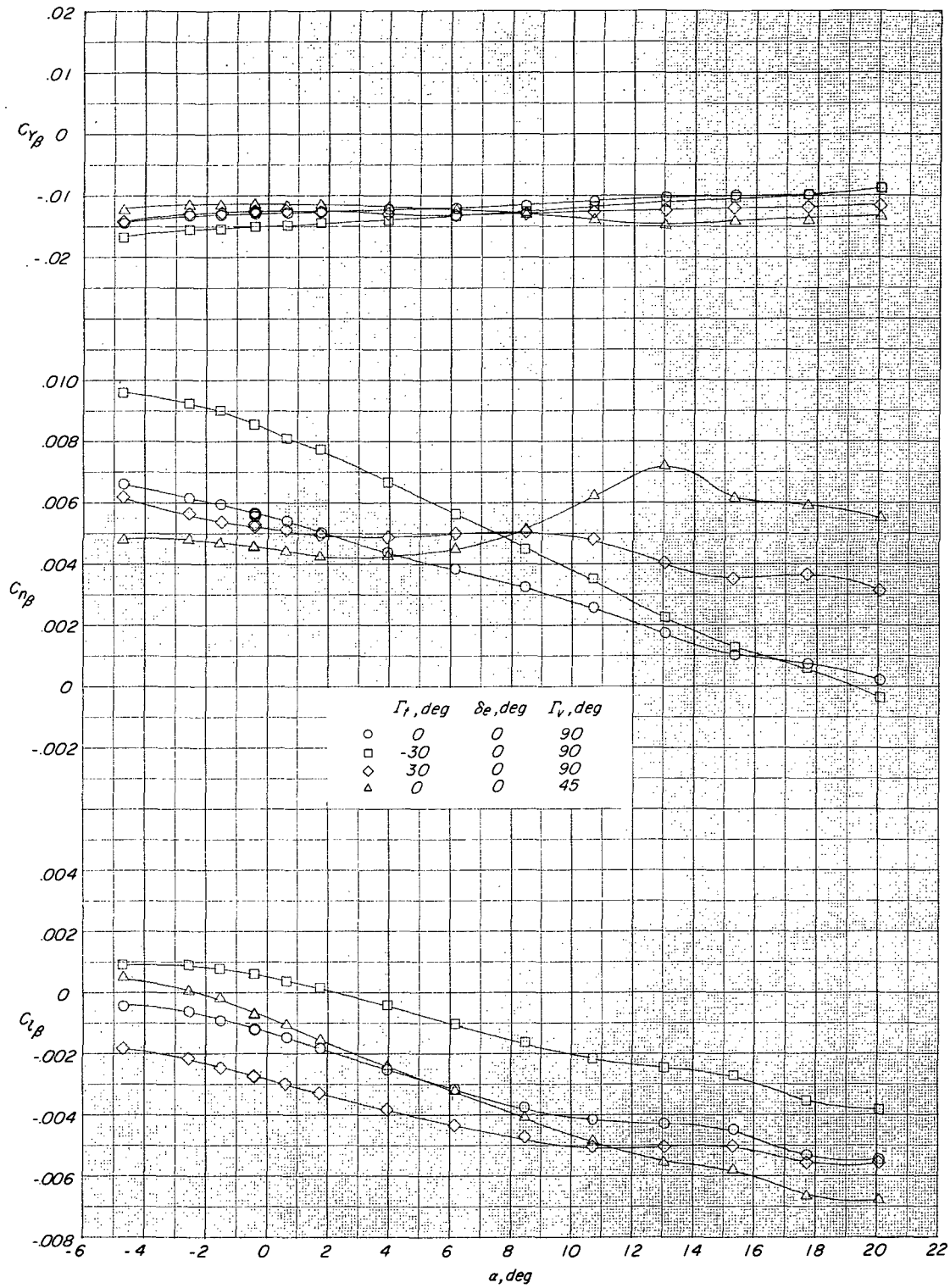

(a) M = 2.30.

Figure 11.- Lateral-directional stability characteristics associated with changes in horizontal-tail dihedral.

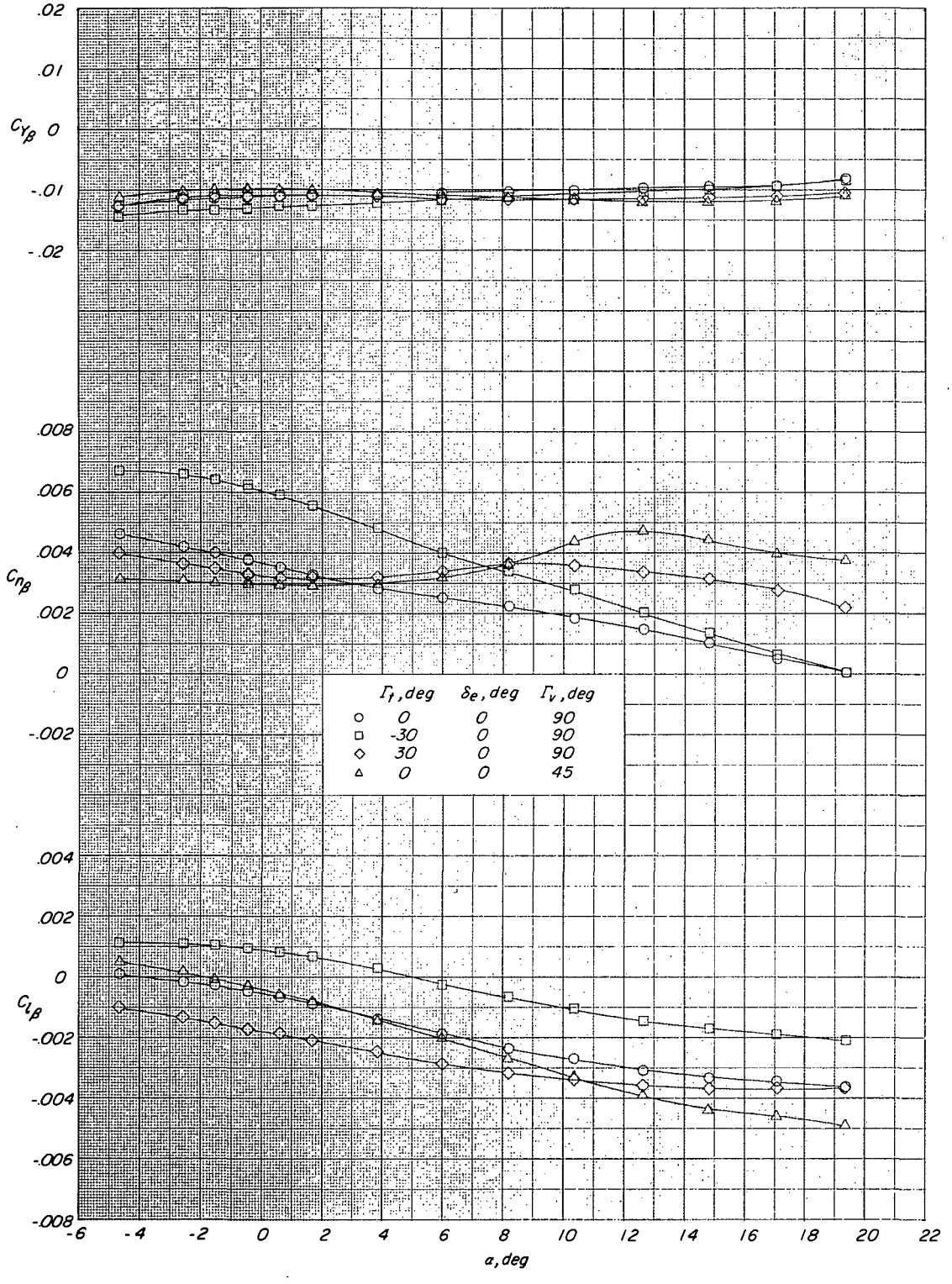

(b) M = 2.96.

Figure 11.- Continued.

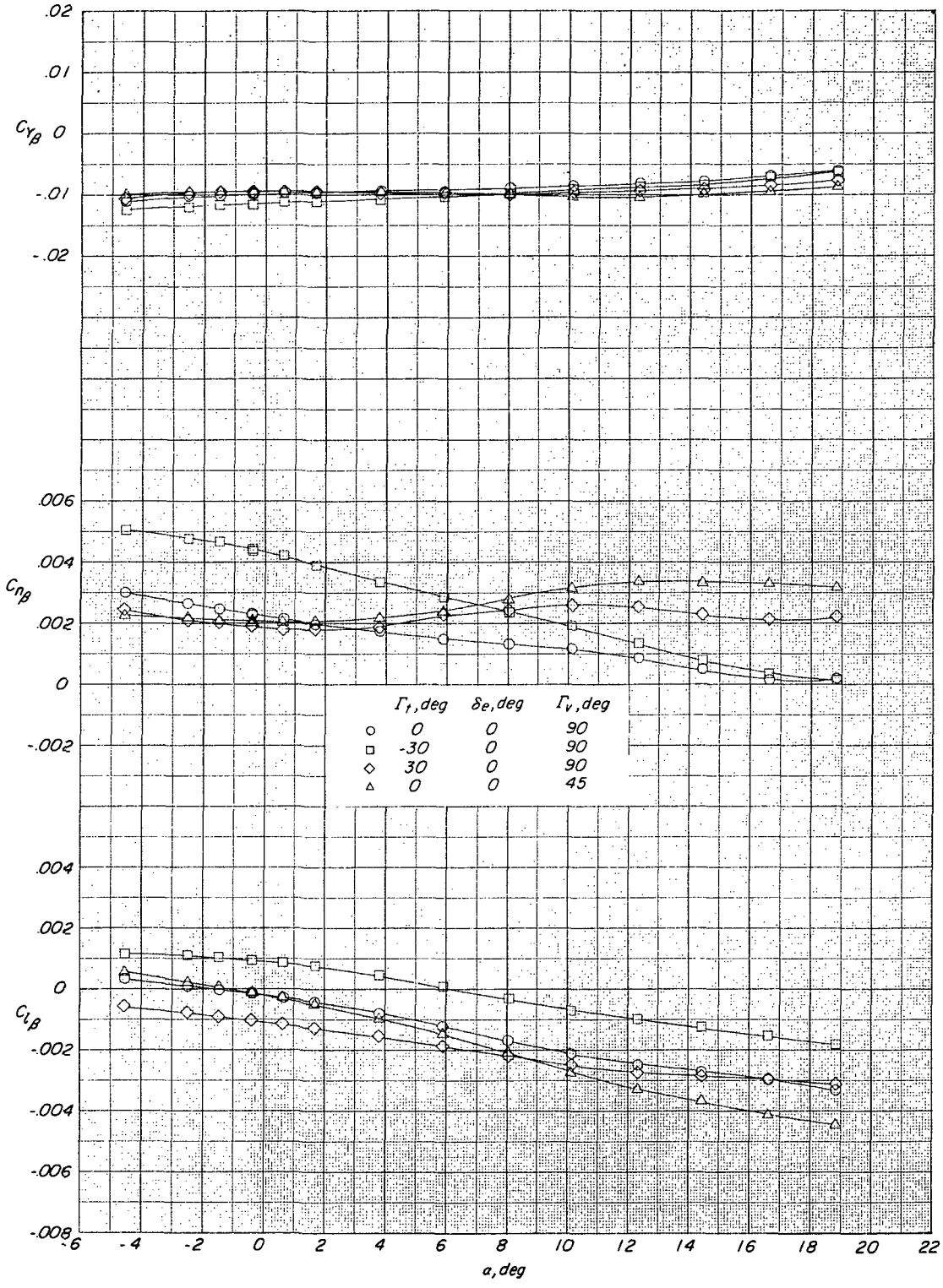

(c) M = 3.96.

Figure 11.- Continued.

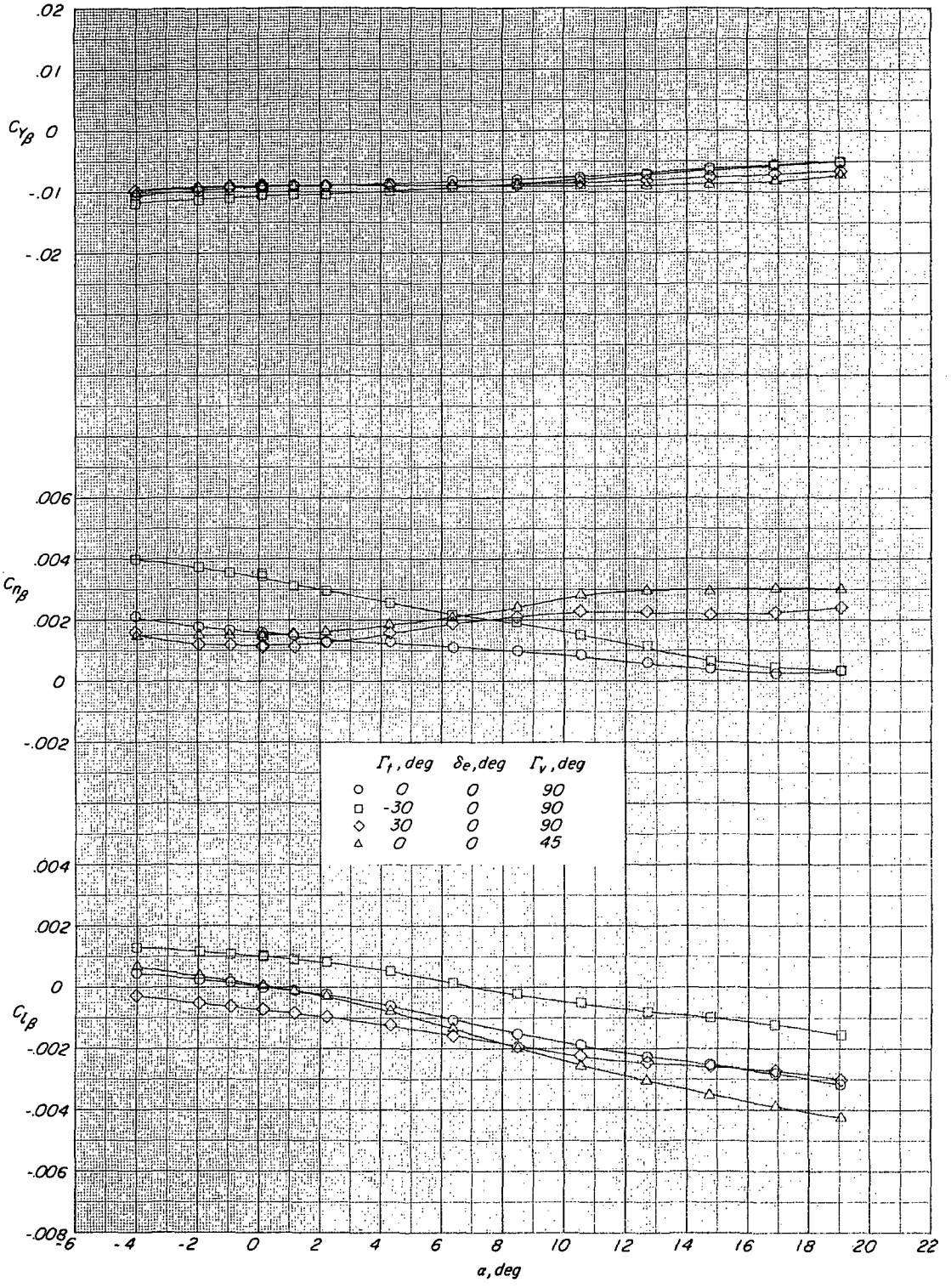

(d) M = 4.63.

Figure 11.- Concluded.

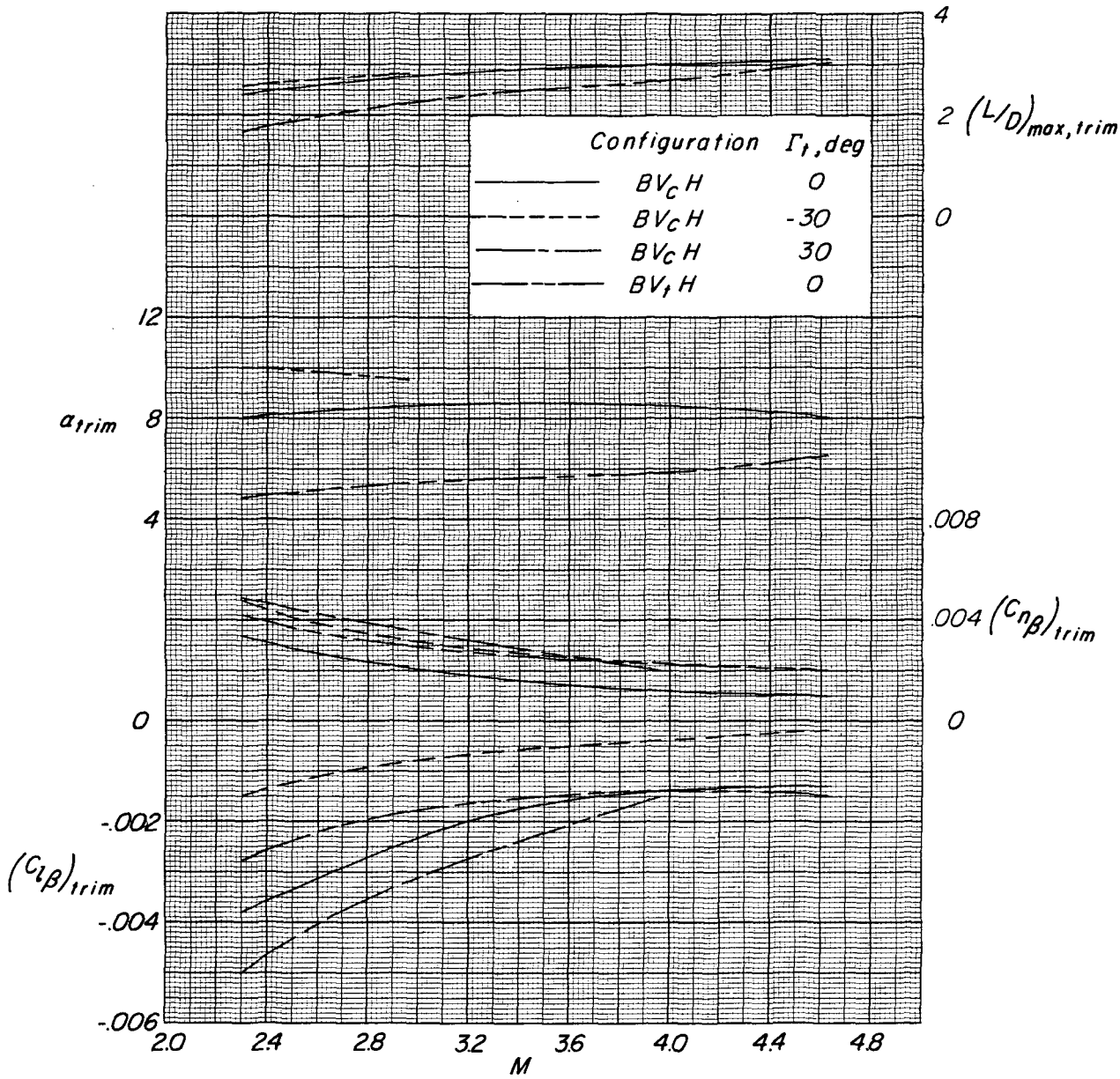

Figure 12.- Summary of aerodynamic characteristics at trim $(L/D)_{max}$ for various configurations.

NASA-Langley, 1973 — 1 L-8639